International Journal of Earth Sciences (2019) 108:2129–2152
https://doi.org/10.1007/s00531-019-01754-2

ORIGINAL PAPER

Kinematics and time of emplacement of the Upper Allochthon of the Rhodope Metamorphic Complex: evidence from the Rila Mountains, Bulgaria

Tsvetelina Gorinova[1] · Neven Georgiev[1] · Zlatka Cherneva[2] · Kalin Naydenov[3] · Valentin Grozdev[3] · Anna Lazarova[3]

Received: 26 October 2018 / Accepted: 13 July 2019 / Published online: 2 August 2019

Abstract

The Rhodope Metamorphic Complex is a nappe pile of four large allochthonous megaunits, referred to as Lower, Middle, Upper, and Uppermost allochthons. These were originally derived from different paleogeographic provinces and were stacked on top of each other in the course of convergent processes along the European continental margin between the Late Jurassic and the Late Eocene. The direction and age of thrusting as well as the degree and age of Alpine metamorphism vary between individual allochthons and are altogether controversial. The affiliation of individual tectonic units to allochthons is often unclear. However, for the area of the Eastern Rhodope Mountains, there is agreement that the thrusting of the Upper Allochthon onto the Middle Allochthon happened before ca. 68–70 Ma, since Upper Cretaceous magmatic bodies crosscut the metamorphic fabric of the rocks. For the northwestern parts of the Rhodope Metamorphic Complex (Rila Mountains), the age of thrusting was considered to predate the Late Cretaceous. Here, we present the results of mapping, structural observations, and LA-ICP-MS dating of zircons and monazites from the Northwest Rila Mountains and revise the tectonic architecture and history of the area. There the boundary between the Upper and Middle allochthons is the Dodov-vrah Shear Zone. This regional-scale structure represents a top-to-the-southeast amphibolite-facies thrust, along which numerous syn-kinematic intrusive bodies were emplaced. U–Pb LA-ICP-MS zircon and monazite dating of the latter, as well as dating of pre- and post-kinematic plutonic rocks from the study area showed that the time of activity of the Dodov-vrah Shear Zone can be bracketed between ca. 58 Ma and 50–48 Ma. Thus, at least for the northwestern parts of the Rhodope Metamorphic Complex, the thrusting of the Upper onto the Middle Allochthon happened after the latest Palaeocene and before the end of the Lower Eocene.

Keywords Rhodope Metamorphic Complex · Compressional tectonics · Late Cretaceous · Shear zones · LA-ICP-MS dating

Electronic supplementary material The online version of this article (https://doi.org/10.1007/s00531-019-01754-2) contains supplementary material, which is available to authorized users.

✉ Tsvetelina Gorinova
tsgorinova@gea.uni-sofia.bg

Neven Georgiev
neven@gea.uni-sofia.bg

Zlatka Cherneva
cherneva@gea.uni-sofia.bg

Kalin Naydenov
naydenov@geology.bas.bg

Valentin Grozdev
vgrozdev@geology.bas.bg

Anna Lazarova
alazarova@geology.bas.bg

[1] Department of Geology, Paleontology and Fossil Fuels, Sofia University "St. Kliment Ohridski", 15 Tzar Osvoboditel Blv, 1000 Sofia, Bulgaria

[2] Department of Mineralogy, Petrology and Economic Geology, Sofia University "St. Kliment Ohridski", 15 Tzar Osvoboditel Blv, 1000 Sofia, Bulgaria

[3] Geological Institute, Bulgarian Academy of Sciences, 1113 Sofia, Bulgaria

Introduction

After decades of studies, the Alpine age of formation of the Rhodope Metamorphic Complex (also Rhodope Massif or Rhodope Zone by different authors) is widely accepted (Fig. 1). Tectonic interpretations agree on the complex (earlier compressional and later extensional) tectono-metamorphic history of the units that compose the Rhodope nappe edifice (Ivanov 1988, 1989; Burg et al. 1990, 1995, 1996; Dinter and Royden 1993; Dinter 1998; Ricou et al. 1998; Burg 2012; Froitzheim et al. 2014). By contrast, the particular characteristics and age of structures within the different units of the Rhodope nappe pile are still poorly known. The complexity of this matter is due to the fact that the rocks and structures related to compressional and extensional processes have recorded similar direction of tectonic transport. Furthermore, thrusts defining the nappe edifice have formed at very different times and yet show similarities in their metamorphic grade and kinematics (Burg et al. 1990, 1995, 1996; Bonev et al. 2006, 2010a, b; Burg 2012; Jahn-Awe et al. 2012; Froitzheim et al. 2014; Georgiev et al. 2016; Ivanov 2017). Therefore, attributing structures to certain compressional events becomes challenging.

With respect to the age of the south-facing, post-Late Jurassic/Early Cretaceous thrusting and subsequent extensional tectonics, two groups of interpretations exist in the literature: (1) the south verging thrusting finished in Late Cretaceous–Earliest Paleocene time. Only after a relatively long period of thermal relaxation, in the Middle Eocene and later, extensional tectonics affected the Rhodope Metamorphic Complex (Burg et al. 1996; Ricou et al. 1998; Bonev et al. 2006; Burg 2012; Sarov 2012). The latter led

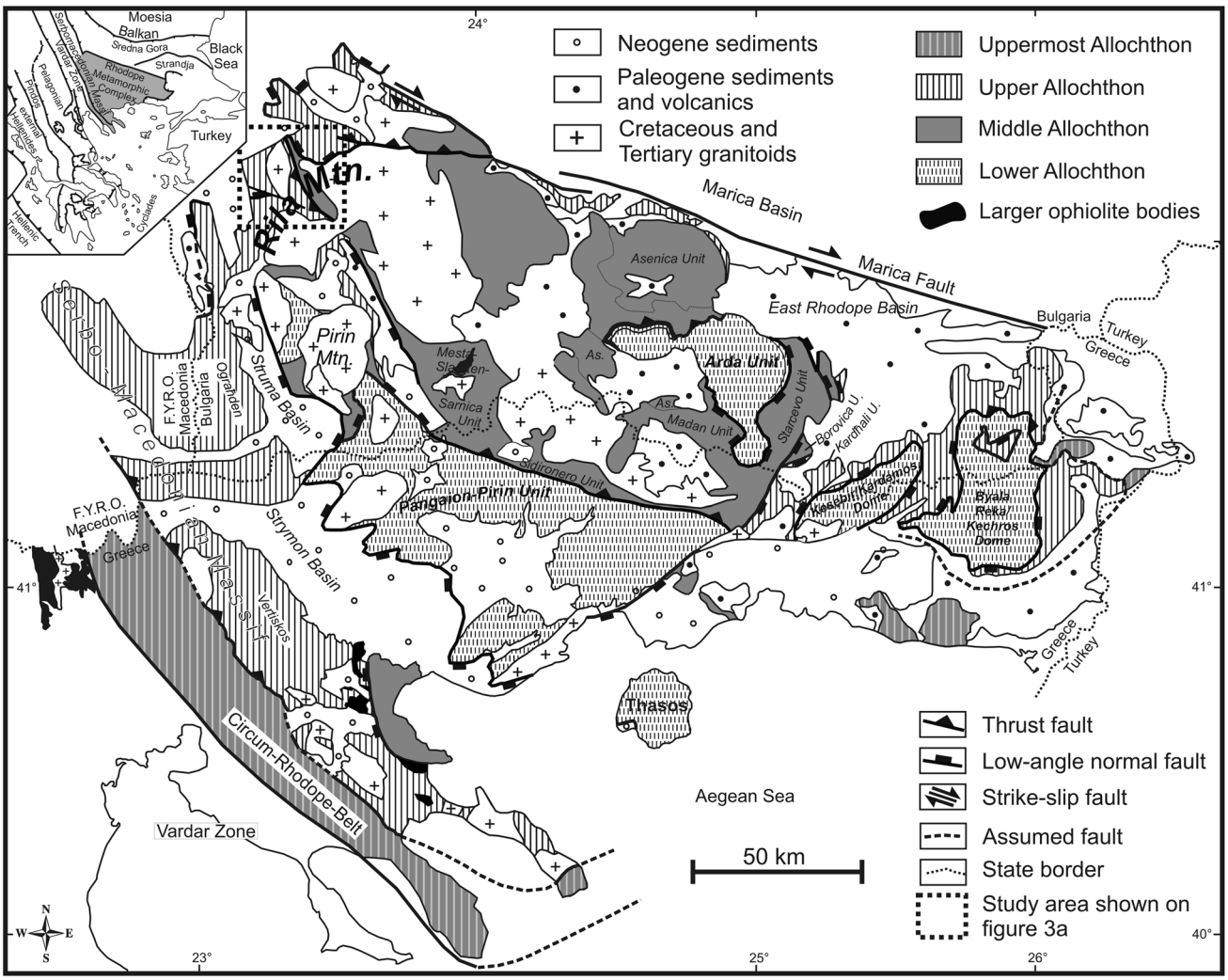

Fig. 1 Tectonic map of the Rhodope Metamorphic Complex (modified after Burg et al. 1996; Ricou et al. 1998; Bonev et al. 2006; Dixon and Dimitriadis 1984)

to the exhumation of high-grade metamorphic rocks along detachment faults and formation of syn-tectonic sedimentary basins and (2) the Late Alpine thrusting finished only in Mid-to-Late Eocene time (Bosse et al. 2009; Jahn-Awe et al. 2010; Nagel et al. 2011; Kirchenbaur et al. 2012; Gautier et al. 2017) and while the south directed compressional regime in the lower parts of the nappe system was still active, the higher parts of the nappe pile underwent an extensional tectonic denudation (Jahn-Awe et al. 2010, 2012; Georgiev et al. 2010; Nagel et al. 2011).

Regional-scale geological setting

Several regional-scale tectonic schemes have been suggested for the Rhodope Metamorphic Complex (Burg et al. 1995; Ricou et al. 1998; Janák et al. 2011; Burg 2012). Below, we follow the interpretation proposed by Janák et al. (2011) and developed further by Jahn-Awe et al. (2012) and Froitzheim et al. (2014). In this interpretation, the Rhodope Metamorphic Complex is considered as composed of four large, orogen-scale allochthonous thrust sheets, namely: Lower, Middle, Upper, and Uppermost Allochthons (Fig. 1).

The different allochthons originated in a specific geodynamic environment as distinct paleogeographic provinces, and were stacked together during a complex convergence history in the northern Tethyan realm from Late Jurassic to Late Eocene times (for details see Janák et al. 2011; Nagel et al. 2011; Jahn-Awe et al. 2012; Froitzheim et al. 2014).

The Uppermost Allochthon, also referred to as Circum–Rhodope Triassic–Jurassic Tectonic Zone in Jaranoff (1960) or Circum–Rhodope Belt in Kauffmann et al. (1976), represents a greenschist- to blueschist-facies thrust sheet derived from a Jurassic volcanic island arc and back-arc setting and formed above a south dipping oceanic subduction zone. In the Late Jurassic–Early Cretaceous, in the course of an arc-continent collision, the Uppermost Allochthon was obducted towards north (Okay et al. 2001; Bonev and Stampfli 2003, 2008) onto the passive European continental margin (i.e., the Upper Allochthon).

The Upper Allochthon represents the European continental margin that was involved in the Early Alpine (Late Jurassic–Early Cretaceous) Orogeny, subducting below and colliding with the Jurassic Arc (i.e., the Uppermost Allochthon) located to the south. The units constituting the Upper Allochthon show a complex polycyclic tectonometamorphic history. They contain remnants (including HP and UPH mineral assemblages) of several orogenies, from Variscan (and probably earlier) to Late Cretaceous (Zidarov et al. 1995; Carrigan et al. 2006; Krenn et al. 2010; Peytcheva et al. 2009; Schmidt et al. 2010; Kirchenbaur et al. 2012; Miladinova et al. 2013; Gorinova et al. 2014; Liati et al. 2015; Georgiev et al. 2016). The regional amphibolite-facies foliation of the Upper Allochthon in the Eastern Rhodopes was formed before Late Cretaceous–Early Paleocene times, since it was crosscut by 69 Ma late-kinematic plutons (Marchev et al. 2006) and ~ 65 Ma post-kinematic granitic dykes (Mposkos and Wawrzenitz 1995). To the southwest, the Vertiskos Unit in Greece, also considered a part of the Upper Allochthon (Janák et al. 2011; Nagel et al. 2011; Jahn-Awe et al. 2012; Froitzheim et al. 2014), underwent shearing after the emplacement of the Triassic Arnea Pluton (Himmerkus et al. 2009). The metamorphic foliation in a small fragment of the Upper Allochthon on the eastern slopes of Pirin Mountains in Bulgaria was crosscut by Upper Cretaceous (85–71 Ma) plutons and mafic dykes (Marchev and Filipov 2012).

The Middle Allochthon is a mixed section of metamorphic rocks of oceanic, arc, and continental origin. Large part of the Middle Allochthon represents a fragment of the former Jurassic arc (i.e., the protoliths of the Uppermost Allochthon) which earlier, in the latest Jurassic, collided with and was obducted onto the Upper Allochthon (Bonev and Stampfli 2003, 2008). Typical for the units comprising the Middle Allochthon are orthogneisses and amphibolites with Late Jurassic magmatic protolith ages and orthogneisses with Early Cretaceous magmatic protolith ages (150–160 Ma and 130–135 Ma, Peytcheva et al. 2007; Von Quadt et al. 2006; Turpaud 2006; Turpaud and Reischmann 2010; Von Quadt et al. 2008; Cherneva et al. 2011; Popov and Ivanov 2012; Froitzheim et al. 2014). The present position of the Middle and Upper allochthons shows that their initial tectonic relationships were disturbed after the Jurassic collision. In the Rhodopes, the Middle Allochthon is located structurally below the Upper Allochthon. The actual nature, age, and kinematics of the major thrust along which the Upper Allochthon was emplaced onto the Middle Allochthon are unknown. In the field, the present-day boundaries between units of these two allochthons represent either Late Eocene–Early Oligocene low-angle extensional detachments or steeper brittle normal faults of Oligocene or later age (Burchfiel et al. 2003; Georgiev et al. 2010; Jahn-Awe et al. 2010, 2012; Pleuger et al. 2011). Thus, the original thrust contact is preserved and recognized in limited localities only.

Mélange zones at the base of the Middle Allochthon comprise rocks affected by polycyclic metamorphism (Mposkos et al. 2010; Gautier et al. 2017), namely: a Mesozoic phase/cycle with an UHP event at ca 200 Ma (Nagel et al. 2011; Petrik et al. 2016); followed by HP granulite melting before 160–140 Ma (Didier et al. 2014; Petrik et al. 2016; Gautier et al. 2017 and reference therein); a Late Cretaceous HP event between 92.7 and 70.5 Ma (Collings et al. 2016); and a Cenozoic cycle with a HP eclogite-facies peak before or at 51–42 Ma (Liati 2005; Kirchenbaur et al. 2012) followed

by amphibolite-facies melting before 40 Ma–36 Ma (Liati 2005; Didier et al. 2014; Gautier et al. 2017).

The units that form the Middle Allochthon can be divided into two large nappes—a lower migmatised, and an upper non-migmatised one. The contacts between the two subunits, in different parts of the Rhodope Mountains in Bulgaria, are interpreted as different extensional shear zones of Middle-to-Late Eocene age (Sarov et al. 2008a, b, c; Yordanov et al. 2008a, b; Pleuger et al. 2011; Jahn-Awe et al. 2012). Limited data on the age of metamorphism in the upper nappe suggest 55 Ma in the northern Rhodope Mountains (von Quadt et al. 2006). The migmatisation of the lower nappe was dated at 60–70 Ma (Cherneva et al. 2006, 2011). Age determinations of crosscutting pegmatites from the same migmatised nappe show that the rocks underwent high-temperature metamorphism before 58–43 Ma (Arnaudov et al. 1990; Raeva et al. 2008; Jahn-Awe et al. 2012). The Middle Allochthon hosts metamorphosed Late Cretaceous (ca. 70 Ma) plutons (von Quadt and Peytcheva 2005), syn-kinematic Late Palaeocene–Early Eocene plutons (Ovtcharova et al. 2004; Sarov et al. 2007; Soldatos et al. 2008; Jahn-Awe et al. 2010) and Late Eocene plutons (Peytcheva et al. 1998; Ovtcharova et al. 2003; Jahn-Awe et al. 2012). The Late Palaeocene–Early Eocene plutons were interpreted as products of melting of orthogneisses with Jurassic protolith ages (Jahn-Awe et al. 2010).

During the Mid-to-Late Eocene, the Middle Allochthon was emplaced toward south onto the passive continental margin of Apulia that forms the Lower Allochthon of the Rhodope Metamorphic Complex (Bosse et al. 2009; Jahn-Awe et al. 2012; Froitzheim et al. 2014).

The Lower Allochthon is exposed in the cores of several large dome structures (Pangaion-Pirin, Arda, Kesebir-Kardamos, and Byala reka-Kehros). These are composed of orthogneisses of Variscan age (280–310 Ma). In some areas a thick layer of marbles overlies the orthogneisses. The marbles were considered as a Mesozoic sedimentary cover (Kronberg 1969; Turpaud and Reischmann 2010; Nagel et al. 2011). Depending on the particular structural position the rocks of the Lower Allochthon are migmatised (Arda and Kesebir-Kardamos domes) or non-migmatised (Pangaion-Pirin and Byala reka-Kehros domes). The migmatisaton in the Arda Dome was dated at 35–38 Ma (Peytcheva et al. 2004 and reference therein).

During the Late Alpine extensional stages (Late Eocene–Oligocene and Mid-Miocene), this quadruple crustal "sandwich", formed by the four allochthons, has been reshaped by low-angle detachment faults and tectonically disrupted into two parts known as the Rhodopean and Serbo–Macedonian massifs.

In this paper, we present new structural, petrological and age data from the Northwest Rila Mountains in Bulgaria (Fig. 1), where the Dodov-vrah Shear Zone represents a preserved segment of the original major thrust along which the Upper Allochthon was emplaced onto the Middle Allochthon. In the discussion, we make a larger scale correlation of the studied structures with other similar regional-scale features over the entire Rhodope Metamorphic Complex.

Tectonic stratigraphy of the study area

Most of the recent studies of the Rila Mountains crystalline basement focused on the Cenozoic exhumation (Shipkova 1999; Dimov and Georgiev 2000; Shipkova and Ivanov 2000; Gerdjikov et al. 2006; Tueckmantel et al. 2008) and only a few papers dealt with its earlier tectono-metamorphic history (Dimov and Damyanova 1996; Kolcheva and Cherneva 1999; Shipkova 1999; Machev P2002). Several papers suggest different tectonic subdivision of the rocks from the metamorphic basement of the Rila Mountains area and distinguished different tectonic units (shown in Fig. 2). According to Shipkova (1999), the boundaries between the units represent top-to-the-southeast syn-metamorphic thrusts. The post-kinematic Kalin Pluton was emplaced along the boundary between Kabul Complex and Karaul migmatites (see Fig. 2) and crosscuts the youngest metamorphic fabric in both units (Sarov et al. 2011a, b, c, d). During the Latest Eocene and Early Oligocene the metamorphic basement of Northwest Rila Mountains was exhumed along the top-to-the-north directed North-Rila Detachment Fault (Gorinova and Georgiev 2015); parts of which were termed Djerman Detachment Fault in Shipkova (1999) and Shipkova and Ivanov (2000), and Rila–Pastra Normal Fault in Tueckmantel et al. 2008). Early Oligocene continental sediments (for regional stratigraphy see Zagorchev et al. 1999) were deposited syn-tectonically onto the hanging wall of the detachment fault.

Based on our field observations, a detailed structural analysis and U–Pb zircon and U–Th–Pb monazite dating of pre-, syn-, and post-kinematic magmatic rocks, we suggest a revision of the existing tectonic subdivisions. We distinguish the following tectonic units in the metamorphic basement of Northwest Rila Mountain: Malyovitsa Unit, representing the Middle Allochthon of the Rhodope Metamorphic Complex, and Kabul, Polich, Sredna Gora and Verila units, representing different structural levels of the Upper Allochthon (Figs. 2, 3a). The boundaries between the five units represent shear zones or faults with different ages, kinematics and metamorphic conditions.

Below, we describe the Malyovitsa Unit, the Kabul Unit and the separating Dodov-vrah Shear Zone in detail as the latter represents the boundary between the Middle and Upper Allochthon (Fig. 3a, b).

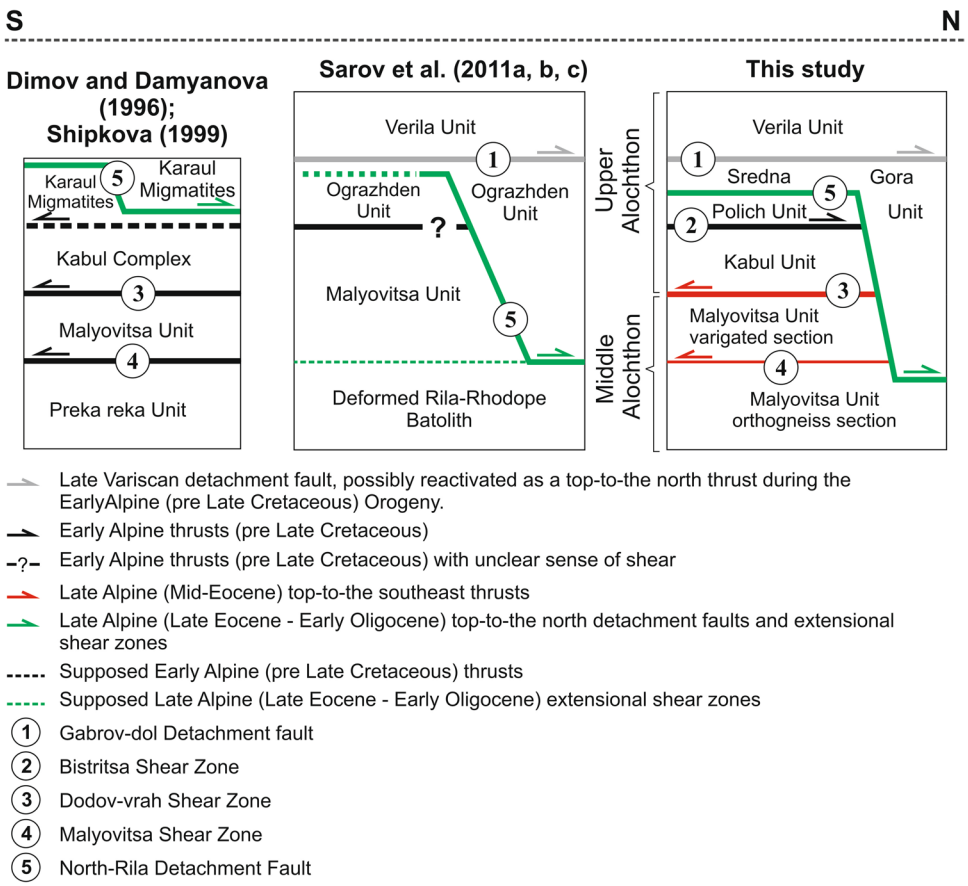

Fig. 2 Comparison between the lithotectonic units of Northwest Rila Mountain and their structural relationships in previous and the current study

Malyovitsa tectonic unit

The Malyovitsa Unit consists of orthogneisses at the base and a variegated section of paragneisses, orthogneisses, amphibolites, marbles, schists and metaultrabasic rocks at the top (Preka-reka orthogneiss Unit and Malyovitsa biotite paragneiss Unit in Dimov and Damyanova 1996; Shipkova 1999, see also Fig. 2). Two top-to-the southeast mylonitic shear zones can be identified (Figs. 2, 3a): (1) the Dodov-vrah Shear Zone at the top and (2) the Malyovitsa Shear Zone, an internal boundary separating the lower orthogneiss from the upper variegated sections (Dimov and Damyanova 1996; Shipkova 1999). The rocks of the unit underwent moderate amphibolite-facies metamorphism (Dimitrova 1960) showing no evidence of high-pressure or high-temperature metamorphism. Microstructural studies and feldspar thermometry for the lower orthogneiss section show that during the last metamorphic event and coeval shearing, the rocks underwent temperatures of 500–550 °C (Cherneva et al. 1998). Foliation and stretching lineation in both the orthogneiss and variegated parts of the section share a common orientation. Similarly, kinematic indicators show identical top-to-the-southeast senses of shear (Dimov and Damyanova 1996; Shipkova 1999, also this study). Popov and Ivanov (2012) reported 135.2 ± 1.0 Ma protolith ages for orthogneisses from the lower structural levels of the Malyovitsa Unit. The age of metamorphism of the unit is not well established. Field relationships between fabrics and dated intrusive rocks show that the main penetrative fabric of the Malyovitsa Unit, affects the Late Cretaceous (70–72 Ma) granodiorite of the Rila–Rhodope Batholith (Von Quadt and Peytcheva 2005; Peytcheva et al. 2007). The penetrative metamorphic foliation is crosscut by post-kinematic, Late Eocene (42–37.5 Ma) granites of the Rila–Rhodope Batholith (Von Quadt and Peytcheva 2005; Peytcheva et al. 2007) providing a minimum age for the main metamorphic fabric.

Kabul tectonic unit

The Kabul Unit is composed of high-grade metamorphic rocks, showing field evidences of migmatisation. The lower structural level of the unit consists of garnet–biotite–kyanite–sillimanite or andalusite–chloritoid-bearing schists, paragneisses and orthogneisses that host large bodies of amphibolite and relics of eclogite. The protolith age of the amphibolites is ca. 265 Ma (Gorinova et al. 2015b) and the relic eclogites yielded a "questionable" (poorly defined) Triassic (~ 235 Ma) metamorphic age (Miladinova et al. 2013). U–Pb zircon dating of garnet-bearing leucosomes in the schists suggested an age of migmatisation of ca.

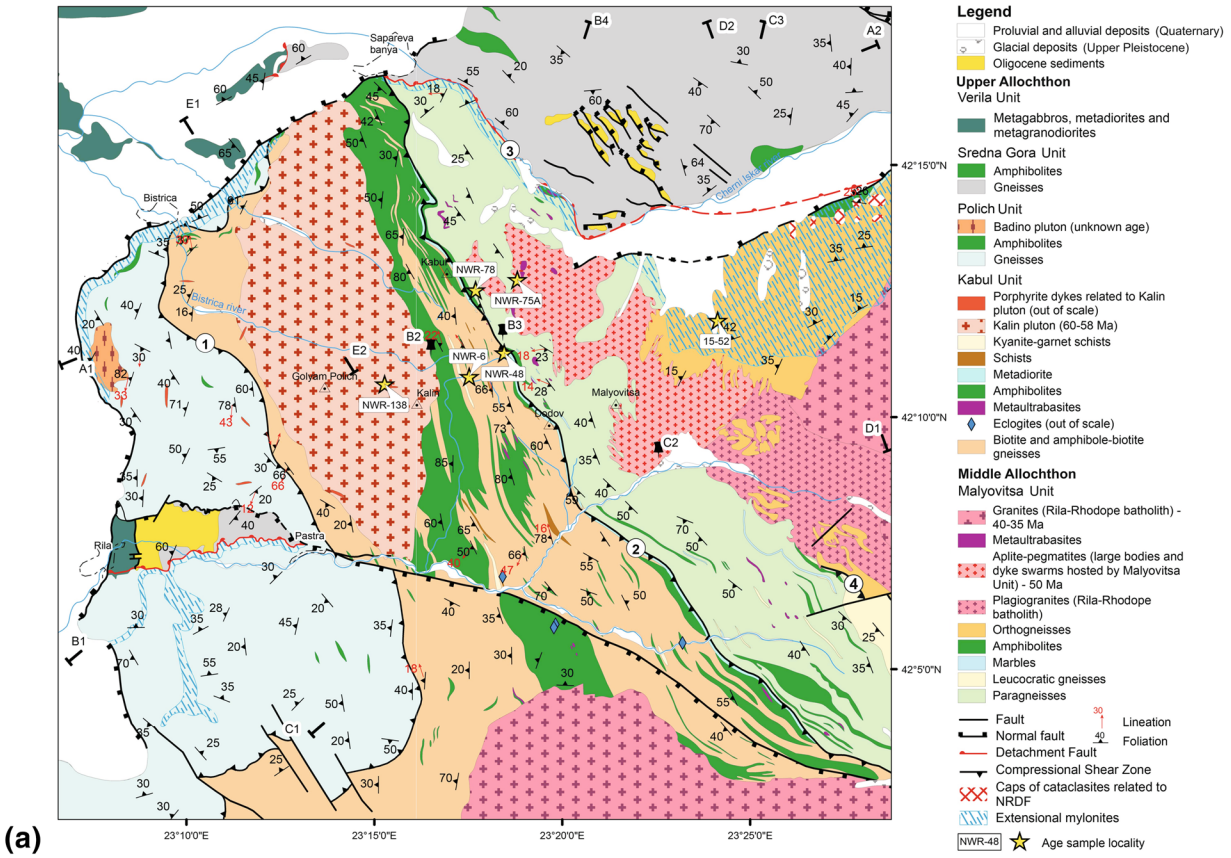
Legend
Proluvial and alluvial deposits (Quaternary)
Glacial deposits (Upper Pleistocene)
Oligocene sediments
Upper Allochthon
Verila Unit
Metagabbros, metadiorites and metagranodiorites
Sredna Gora Unit
Amphibolites
Gneisses
Polich Unit
Badino pluton (unknown age)
Amphibolites
Gneisses
Kabul Unit
Porphyrite dykes related to Kalin pluton (out of scale)
Kalin pluton (60-58 Ma)
Kyanite-garnet schists
Schists
Metadiorite
Amphibolites
Metaultrabasites
Eclogites (out of scale)
Biotite and amphibole-biotite gneisses
Middle Allochthon
Malyovitsa Unit
Granites (Rila-Rhodope batholith) - 40-35 Ma
Metaultrabasites
Aplite-pegmatites (large bodies and dyke swarms hosted by Malyovitsa Unit) - 50 Ma
Plagiogranites (Rila-Rhodope batholith)
Orthogneisses
Amphibolites
Marbles
Leucocratic gneisses
Paragneisses
Fault
Normal fault
Detachment Fault
Compressional Shear Zone
Caps of cataclasites related to NRDF
Extensional mylonites
Lineation
Foliation
NWR-48 Age sample locality
Bistrica
Sapareva banya
Kabul
Golyam Polich
Malyovitsa
Dodov
Pastra
Rila
Otmen
NWR-78
NWR-75A
NWR-6
NWR-48
NWR-138
15-52
42°15'0"N
42°10'0"N
42°5'0"N
23°10'0"E
23°15'0"E
23°20'0"E
23°25'0"E

(a)

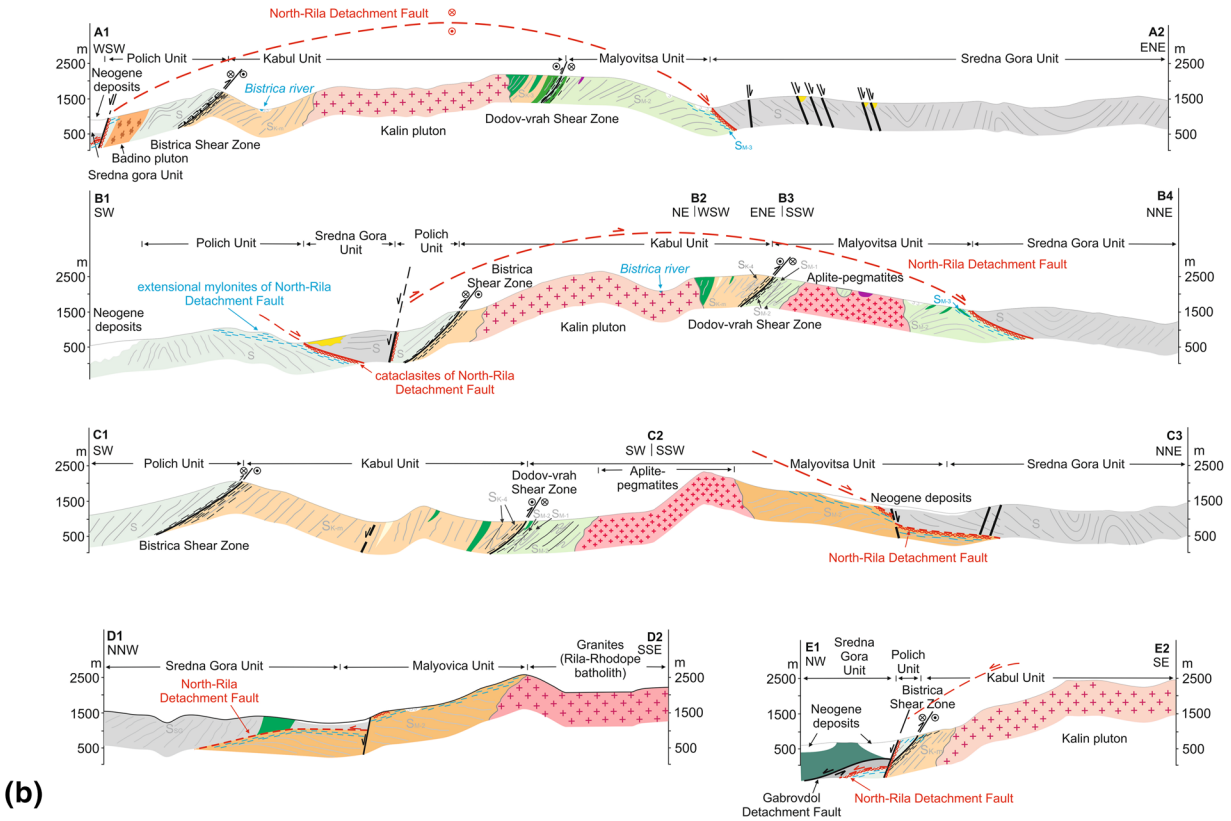
North-Rila Detachment Fault
A1
WSW
Polich Unit
Kabul Unit
Malyovitsa Unit
Sredna Gora Unit
A2
ENE
Neogene deposits
Bistrica river
Kalin pluton
Dodov-vrah Shear Zone
Bistrica Shear Zone
Badino pluton
Sredna gora Unit
B1
SW
B2
NE | WSW
B3
ENE | SSW
B4
NNE
Sredna Gora Unit
Polich Unit
extensional mylonites of North-Rila Detachment Fault
Aplite-pegmatites
cataclasites of North-Rila Detachment Fault
C1
SW
C2
SW | SSW
C3
NNE
Aplite-pegmatites
Neogene deposits
D1
NNW
Granites (Rila-Rhodope batholith)
D2
SSE
North-Rila Detachment Fault
E1
NW
E2
SE
Gabrovdol Detachment Fault
m
2500
1500
500

(b)

◂**Fig. 3** **a** Tectonic map of the Northwest Rila Mountain. The numbered circles denote: Bistritsa Shear Zone (1); Dodov-vrah Shear Zone (2); North-Rila Detachment Fault (3); Malyovitsa Shear Zone (4). A1-A2, B1-B2-B3-B4, C1-C2-C3, D1-D2, E1-E2 cross sections shown on **b**. **b** Geological cross sections across Northwest Rila Mountain (refer to **a**)

238 Ma (Gorinova et al. 2015a). The higher structural level is composed of garnet amphibolites (Fig. 7a) with U–Pb zircon protolith ages of ca. 537 Ma (Gorinova and Georgiev 2015). The ages of the subsequent metamorphic events of the Kabul Unit are unknown. The unit hosts meta-diorites to metagabbro-diorite bodies with protolith ages of ca. 76 Ma (Gorinova et al. 2015b; also sample NWR-48 in this study). The main metamorphic fabric is sealed by the Palaeocene (58–60 Ma) granitoid Kalin Pluton (Zagorchev et al. 2014; also sample NWR-138 in this study) and pegmatite dykes of ca. 50 Ma (Arnaudov et al. 1974; Arnaudov 1975). Some of the previous studies have established a clockwise PT evolution culminating at granulite to high amphibolite-facies conditions followed by exhumation to lower amphibolite and greenschist-facies retrogression (Kolcheva and Cherneva 1999; Machev 2002).

Dodov-vrah Shear Zone

The Dodov-vrah Shear Zone is described as a top-to-the-southeast, high-grade shear zone, along which the migmatised Kabul Complex was emplaced on top of the non-migmatic Malyovitsa Unit (Dimov and Damyanova 1996; Shipkova 1999). These studies suggest an Early Alpine age of thrusting (earliest Late Cretaceous). However, no detailed kinematic analyses or absolute dating narrowing the age of thrusting have been performed so far.

Results

Structural data

Malyovitsa Unit

In the bulk of the Malyovitsa Unit, alternating layers of marbles, schists, paragneisses, amphibolites and rarely orthogneisses (Fig. 4b, c) display an isoclinally folded older metamorphic fabric S_{M-1} (*M* is for Malyovitsa Unit). Folds display a new axial planar foliation S_{M-2} defined by feldspar, feldspar–quartz aggregates and phyllosilicates (Fig. 4a). The S_{M-2} foliation represents the main penetrative fabric in the unit. It dips with moderate angles (20°–45°) towards southwest or west (Fig. 5a) and contains a stretching lineation L_{M-2}. The stretching lineation is defined by elongated quartz ribbons, feldspar clasts with pressure shadows or elongated quartz–feldspar aggregates, mica flakes or aligned amphibole crystals. The L_{M-2} is northwest–southeast oriented and parallel to the fold axes of the isoclinal folds (Fig. 5a). The kinematic indicators show a consistent top-to-the-southeast sense of shear (Fig. 6b). The microstructures show that the temperature of formation of S_{M-2} and L_{M-2} was in the field of the amphibolite-facies. Grain boundary migration recrystallization in quartz (Fig. 6a, b) and core-and-mantle structures in feldspar point to a process of dynamic recrystallization at temperatures of ~ 600 °C (Passchier and Trouw 2005; Trouw et al. 2010). In the northern part of the study area, in the vicinity of the shear zone of the North-Rila Detachment Fault (Fig. 3a, b), a lower grade north dipping mylonitic foliation S_{NRD} and related stretching lineation L_{NRD} (NRD is for North-Rila Detachment Fault) overprinted S_{M-2} and L_{M-2} (Figs. 4d, 5b). The microstructural characteristics of quartz, feldspar and micas show that S_{NRD} and L_{NRD} were formed at temperatures of ~ 400–500 °C (Fig. 6c, d). The kinematic indicators, within and close to the North-Rila Detachment Fault, show a consistent top-to-the-north-northwest sense of shear (Fig. 6c, d). Remnants of the brittle section of the detachment fault occupy top parts of north–south elongated ridges in the northern slopes of the Rila Mountains and thus, form klippen-like cataclastic caps (Fig. 3a). Later in the course of Miocene–Quaternary extensional tectonics, large parts of the detachment-related tectonites were overprinted and sheared off by normal faults in the northern, northwestern and western slopes of the Rila Mountains (Fig. 3a, b).

Kabul Unit

The main penetrative deformational fabric in the rocks of the unit is a metamorphic foliation S_{K-m} (*K* for Kabul Unit and *m* for main), which due to the presence of open to tight northeast verging folds dips at 20°–80° to the southwest or northeast. Fold axes plunge with small angles to the northwest or southeast. The foliation bears a stretching lineation L_{K-m} defined by aligned amphiboles and micas as well as stretched quartz and quartz–feldspar aggregates. The stretching lineation is mostly northwest–southeast oriented but due to the later folding it may show deviations (Fig. 8a). The main metamorphic fabrics of the unit were formed at a temperature range of 500–650 °C (Fig. 9a, b). In areas where the foliation and stretching lineation are less folded, reliable kinematic indicators show top-to-the-north-northwest sense of shear (Fig. 7a, b). The upper boundary of the unit represents the regional-scale Bistritsa Shear Zone (Sarov et al. 2011a, d) along which the Kabul Unit is juxtaposed to the overlying amphibolite-facies Polich Unit. The Bistritsa Shear Zone shows similar deformation conditions and kinematics as the S_{K-m}–L_{K-m} fabrics (Fig. 7c). Due to folding (Fig. 7d), the mylonitic foliation dips at 30°–80° to the southwest (Fig. 8b). The related stretching lineation

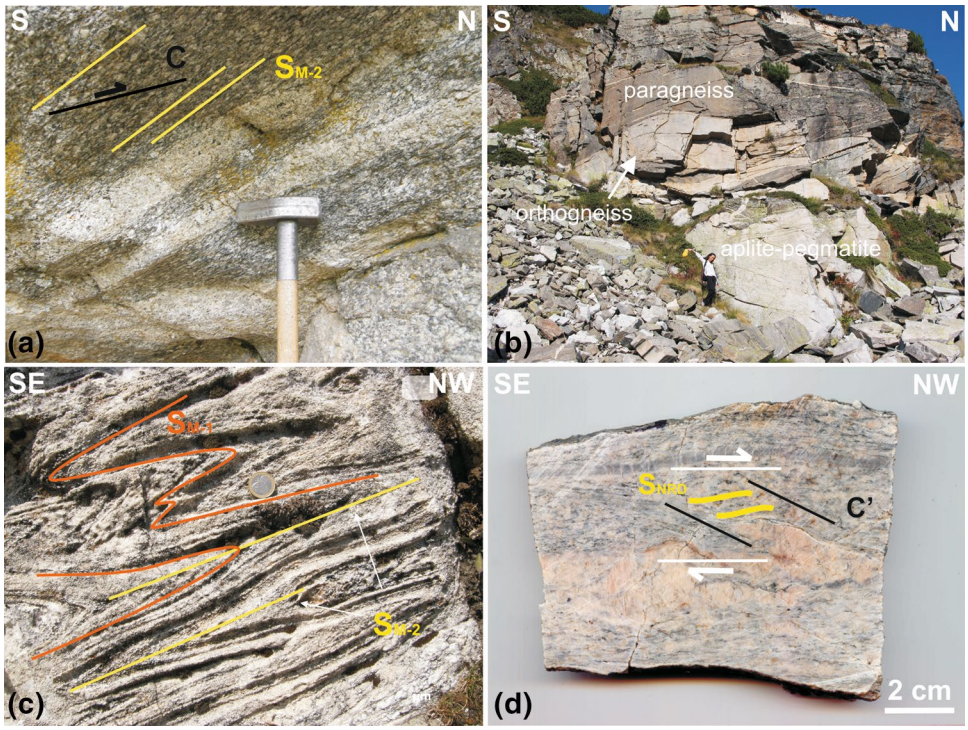

Fig. 4 Rocks and structures of Malyovitsa Unit: **a** S_{M-2}-C fabric in a coarse-grained orthogneiss within the lower section of the unit; **b** orthogneiss body in the paragneisses in the upper section of the unit. An aplite–pegmatite body crosscuts the gneisses. Sample NWR-75A is collected from the orthogneiss body; **c** isoclinally folded S_{M-1} forms the main foliation S_{M-2} in marbles in the upper section of the unit; **d** S_{NRD}-C-C' fabric in the biotite-bearing orthogneiss in the vicinity of the North-Rila Detachment Fault. The kinematic criteria show a top-to-the northwest sense of shear

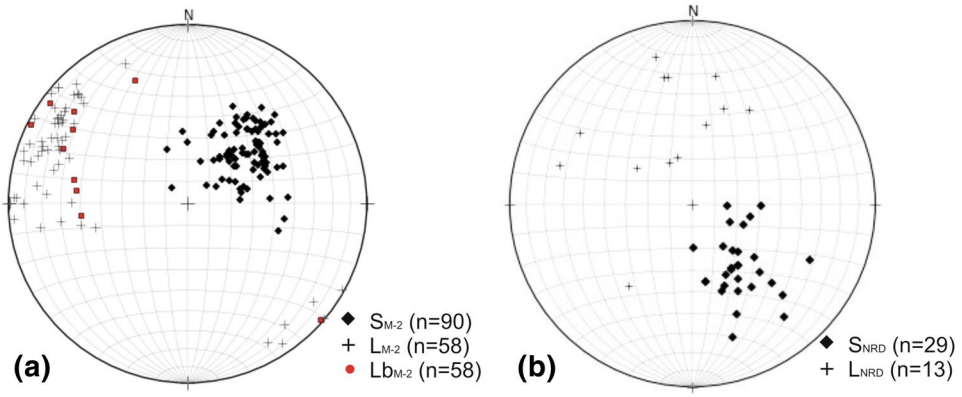

Fig. 5 Lower hemisphere equal area stereoplots: **a** main metamorphic fabric of Malyovitsa Unit—penetrative foliation (S_{M-2}), stretching lineation (L_{M-2}) and fold axes (Lb_{M-2} of isoclinally folded S_{M-1}; **b** mylonitic fabric of North-Rila Detachment foliation (S_{NRD}) and stretching lineation (L_{NRD})

is mostly northwest–southeast oriented but deviations due to folding are also present (Fig. 8b). On the north slopes of the Rila Mountains the high-grade fabric of the Kabul Unit was overprinted and even obliterated by the extensional mylonites of the North-Rila Detachment Fault.

Dodov-vrah Shear Zone

The Dodov-vrah Shear Zone forms a 100–200 m thick domain of intensely sheared rocks, moderately dipping to southwest or west at the boundary between the Malyovitsa and Kabul units. Although the deformation affected rocks of both the footwall and the hanging wall (Fig. 7d), the lower unit (Malyovitsa Unit) accommodated most of it and its rocks received larger amounts of strain. The mylonitic foliation bears a nearly horizontal, northwest–southeast oriented stretching lineation (Fig. 11a). A number of syn-to-late-kinematic granitic veins were emplaced within the shear zone (Fig. 10b). Asymmetric boudinage and folding of veins indicate a top-to-the southeast sense of shear (Fig. 10a, b). Dykes and veins of the same composition also cut the foliation, filling tension gashes that remain almost undeformed and thus, indicating late-kinematic emplacement (Fig. 10b). U–Th–Pb monazite dating of such a syn-to-late-kinematic granite vein (sample NWR-78 in this study, see location in Fig. 3a) was used to determine the age of the Dodov-vrah Shear Zone.

Dynamic recrystallisation of quartz associated with grain boundary migration (Fig. 11b), elongated ribbons of coarsely recrystallised quartz, ribbons of fine-grained,

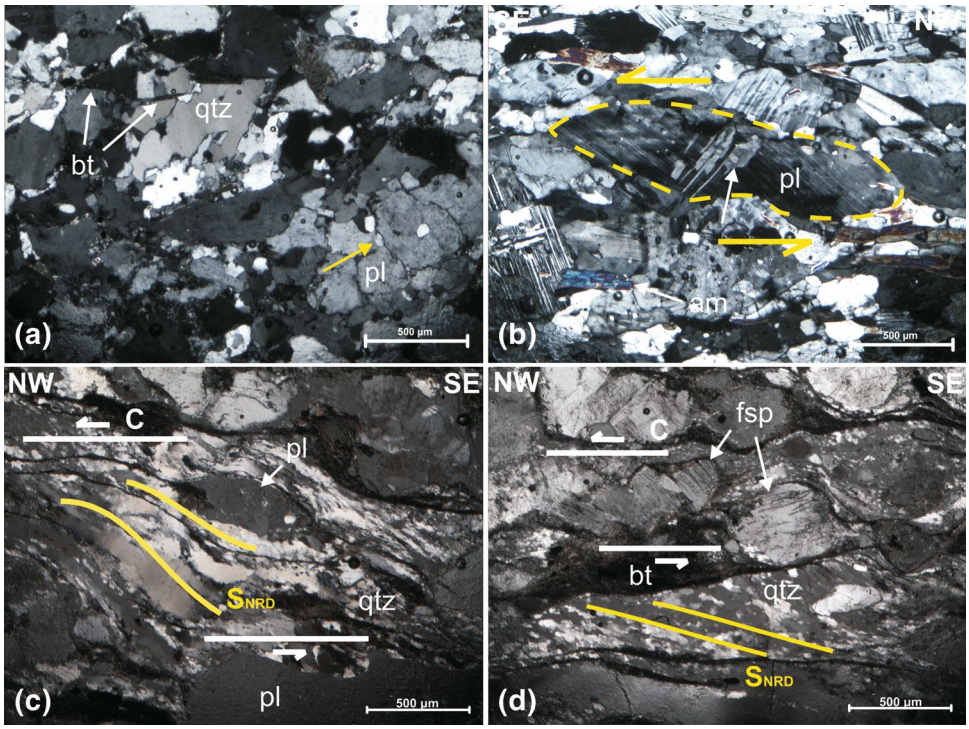

Fig. 6 Microphotographs of samples from the Malyovica Unit in cross-polarized light: **a** lobate grain boundaries of quartz due to grain boundary migration recrystallization typical for the deformation in an amphibolite facies (orthogneiss from the upper section of the unit, close to the Dodov-vrah Shear Zone); **b** thin deformation twin lamellae synthetically oriented with the sinistral shear direction (yellow arrow) and thick deformation twin lamellae, antithetically oriented with the shearing (white arrow) in a lens-shaped plagioclase. The kinematic indicators record top-to-the southeast shearing (amphibole-bearing orthogneiss from the upper section of the unit, close to the Dodov-vrah Shear Zone); **c** monomineral ribbons of elongated and bended large quartz grains surrounded by small quartz grains formed by subgrain rotation recrystallization under greenschist-facies conditions. Thin biotite bands bound quartz ribbons. Lens-shaped plagioclase and bended ribbons indicate top-to-the northwest sense of shearing (mylonitised orthogneiss from the lower section of the unit, deformed in the vicinity of North-Rila Detachment Fault); **d** monomineral ribbon of equigranular quartz grains formed by subgrain rotation recrystallization during greenschist-facies deformation. Domino-type fragmented feldspar porphyroclast and the orientation of quartz subgrains indicate top-to-the northwest sense of shearing (mylonitised orthogneiss from the lower section of the unit, deformed in the vicinity of North-Rila Detachment Fault). Mineral abbreviations by Kretz (1983)

recrystallized feldspar and core-and-mantle structure in plagioclase (Fig. 11c) indicate deformation temperatures of 600–620 °C (Passchier and Trouw 2005; Trouw et al. 2010). The deformation temperatures and kinematics are similar to those of the rocks in the footwall (i.e., Malyovitsa Unit). Therefore, we interpret the mylonitic fabric of the Dodov-vrah Shear zone as equal to that of the Malyovitsa Unit and we denote the mylonitic foliation of the shear zone as S_{M-2} and the related stretching lineation as L_{M-2}.

Close to the Dodov-vrah Shear Zone, the S_{K-m} foliation of the Kabul Unit is isoclinally folded, with fold axes parallel to the stretching lineation in the shear zone. There the S_{K-m} is dragged into parallelism with the mylonitic fabric of the shear zone. Within the shear zone, the older metamorphic fabric of the rocks from the Kabul Unit is reworked by the mylonitic foliation of the Dodov-vrah Shear Zone (i.e., S_{M-2}). There the related kinematic indicators show a consistent top-to-the southeast sense of shear corresponding to the kinematics of the shear zone (Fig. 10a, b).

In the northern slopes of the Rila Mountains (Fig. 3a, b) the high-grade fabric of Dodov-vrah Shear Zone was overprinted by top-to-the-north lower grade mylonitic structure (S_{NRD} and L_{NRD}) of the North-Rila Detachment Fault. Dynamic recrystallisation of quartz associated with subgrain rotation and later bulging (Fig. 11d), formation of flame-perthite, brittle deformation of feldspar, and replacement of biotite by chlorite show that the temperatures of deformation related to the detachment faulting were in the range of 300-400 °C (Passchier and Trouw 2005; Trouw et al. 2010).

Zircon and monazite dating

To assess the time of thrusting along the Dodov-vrah Shear Zone, we applied LA-ICP-MS U–Th–Pb dating of zircons and monazites, extracted from meta-igneous and igneous rocks that were emplaced in the Dodov-vrah Shear Zone and also in its footwall and hanging wall. Zircon and

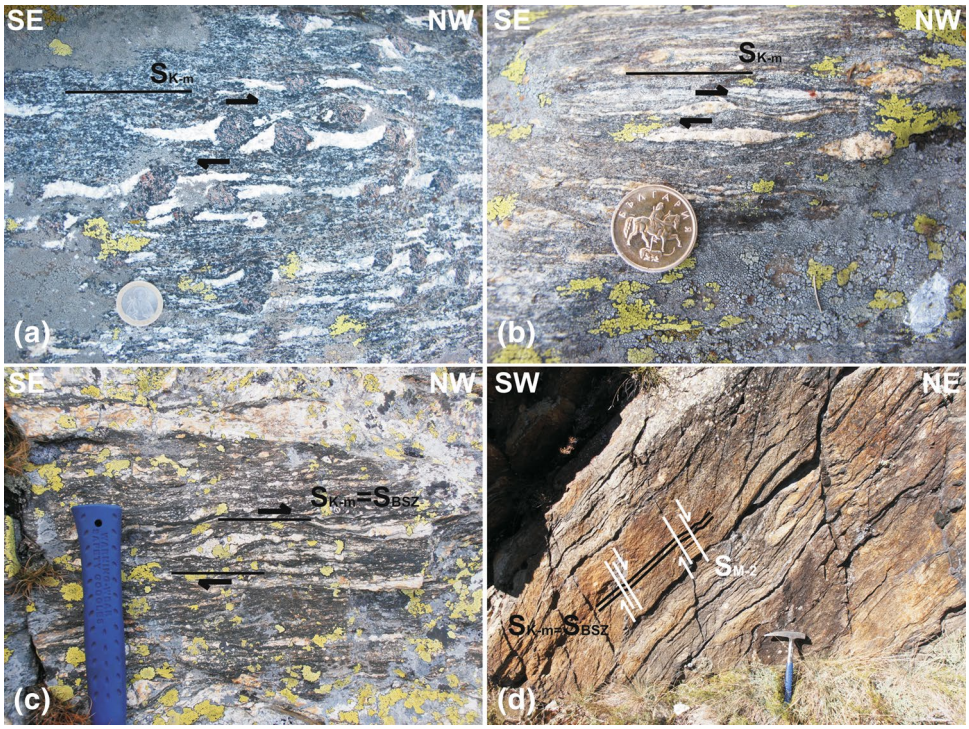

Fig. 7 Rocks and structures of Kabul Unit: **a** garnet-bearing amphibolite in the higher structural level of the unit. The leucosome in the pressure shadows of the garnet porphyroblasts and in patches in the rock is a product of the migmatisation. The pressure shadows show a top-to-the northwest sense of shear; **b** migmatised biotite gneiss from the lower structural levels displays a top-to-the northwest sense of shear; **c** sigma clast of quartz–feldspar aggregate in the amphibole–biotite gneisses of Kabul Unit. The shearing is caused by the movement along Bistritsa Shear Zone. The tectonic transport direction is top-to-the-northwest. The location is south of the Rilska river; **d** a crenulation cleavage synchronous to the formation of S_{M-2} foliation within Dodov-vrah Shear Zone and Malyovitsa Unit and parallel to the fold axes of the main folds in the amphibole–biotite gneisses of Kabul Unit. The folding is caused by the movement along the Dodov-vrah Shear Zone (the location is north of Padala village)

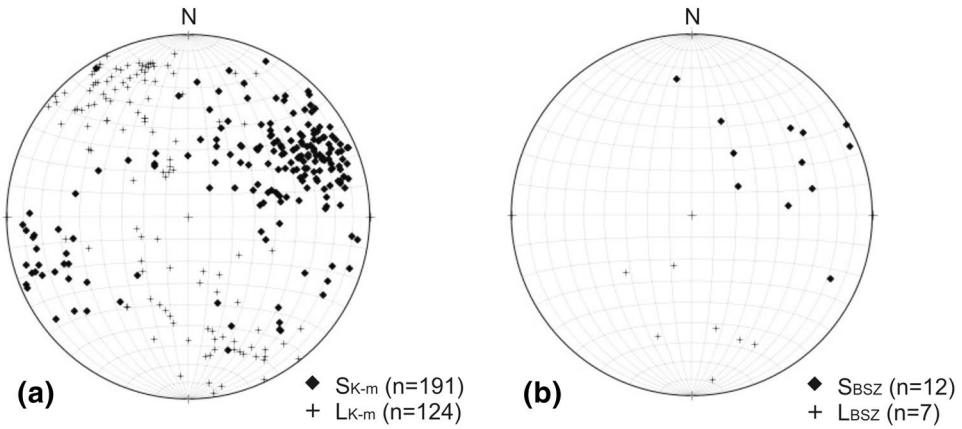

Fig. 8 Lower hemisphere equal area stereoplots of: **a** main metamorphic foliation (S_{K-3}) and stretching lineation (L_{K-3}) related to the amphibolite-facies deformation of Kabul Unit; **b** metamorphic foliation (S_{BSZ}) and stretching lineation (L_{BSZ}) of the Bistritsa Shear Zone

monazite crystals were extracted from the rock samples by standard mineral separation techniques—grinding, Wilfley table, heavy liquids and magnetic separation. Selected crystals were mounted in pellets of epoxy resin, the surfaces of which were sanded down with a diamond paste to expose the interior portions of the grains. All procedures were performed at the Geological Institute of the Bulgarian Academy of Science. To identify the internal structure of the crystals, cathodoluminescence (CL) and back scattered electron (BSE) images were taken with a JEOL JMS-6610 LV SEM–EDS facility at the University of Belgrad, Faculty of Mining and Geology. In-situ U–Th–Pb isotope analyses were performed using a New Wave Research (NWR) 193 nm excimer laser UP-193FX attached to a Perkin-Elmer

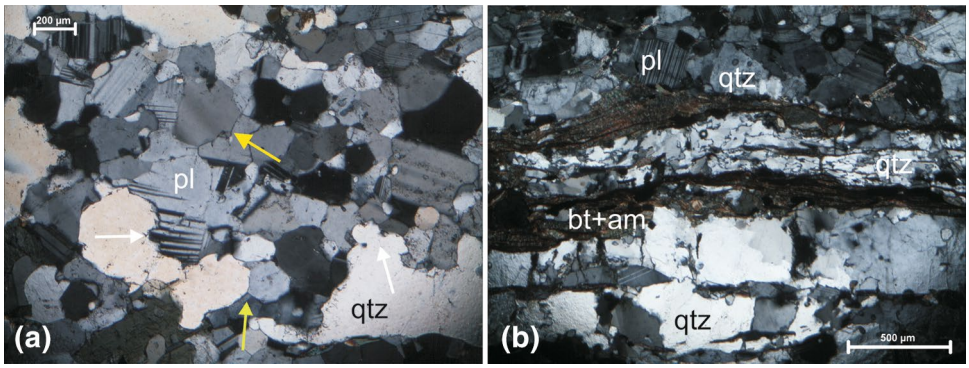

Fig. 9 Microphotographs of samples from the Kabul Unit in cross-polarized light: **a** lobate grain boundaries of quartz and plagioclase formed by grain boundary migration dynamic recrystallization (white arrows) in a leucosome patch in the garnet-bearing amphibolite (from Fig. 7a). GBM was overprinted by static recrystallization during annealing displayed by the polygonal texture of the grains (green arrow). The high-grade structures are overprinted by low-grade structure—deformational lamellae in plagioclase (white arrow) and a weak undulatory extinction of quartz (yellow arrow); **b** alternating quartz and quartz–plagioclase layers in an amphibole–biotite gneiss. The lobate grain boundaries of quartz in the bottom layer are typical for high-grade amphibolite deformation, whereas the quartz subgrains in the center layer display subgrain rotation recrystallization common for a lower grade greenschist facies

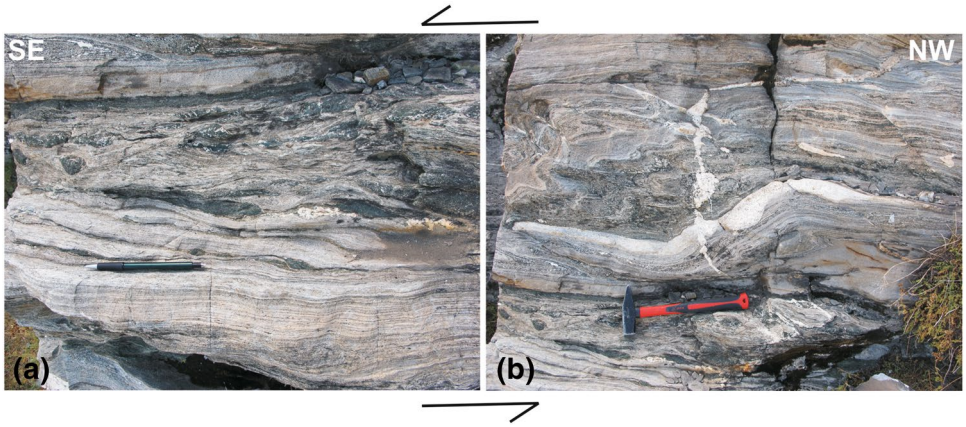

Fig. 10 Structures in the Dodov-vrah Shear Zone near the locality of sample NWR-78: **a** sheared amphibole layer and S_{DSZ}–C_{DSZ} fabric displaying a top-to-the southeast tectonic transport direction in paragneisses of the Malyovica Unit; **b** boudinaged mesocratic layer (in the upper part of the photo) and a vein of granitic composition (in the center) are compressed in the direction of the top-to-the-southeast tectonic transport along the Dodov-vrah Shear Zone. The last one is crosscut by an undeformed pegmatitic vein (vertical). The sample NWR-78 is from a similar late-kinematic vein

ELAN DRC-e quadrupole inductively coupled plasma mass spectrometer (LA-ICP-MS) at the Geological Institute of the Bulgarian Academy of Science. The spot size for zircon was 35 µm, with an energy density of 8.8 J/cm^2 and a repetition rate of 8 Hz. The zircon GJ1 standard (Jackson et al. 2004) was used for fractionation corrections and the Plesovice standard (Slama et al. 2008) as the "unknown". For monazite, the spot size was 10 µm with an energy density of 2.26 J/cm^2 and a repetition rate of 3 Hz. The Moacir monazite standard (Seydoux-Guillaume et al. 2002a, b) was used for fractionation corrections and the 44,069 monazite standard (Aleinikoff et al. 2006) as the "unknown". The common lead (^{204}Pb) was not measured and no Pb correction was applied. Data have been processed with GLITTER 4.0 (Macquarie University, Griffin et al. 2008) software. For each sample, all concordant data were used to calculate a mean age and a concordia age (Wetherill 1956) using ISOPLOT/Ex. 3.22 (Ludwig 2012) software.

Age constrains for the Malyovitsa Unit

Sample NWR-75A (N42°12′56.27″, E23°19′11.39″) was collected from an orthogneiss body situated within paragneisses and schists in the upper section of the Malyovitsa Unit (Fig. 3a, 4b). The zircon population is dominated by euhedral to subhedral short-prismatic grains. The internal

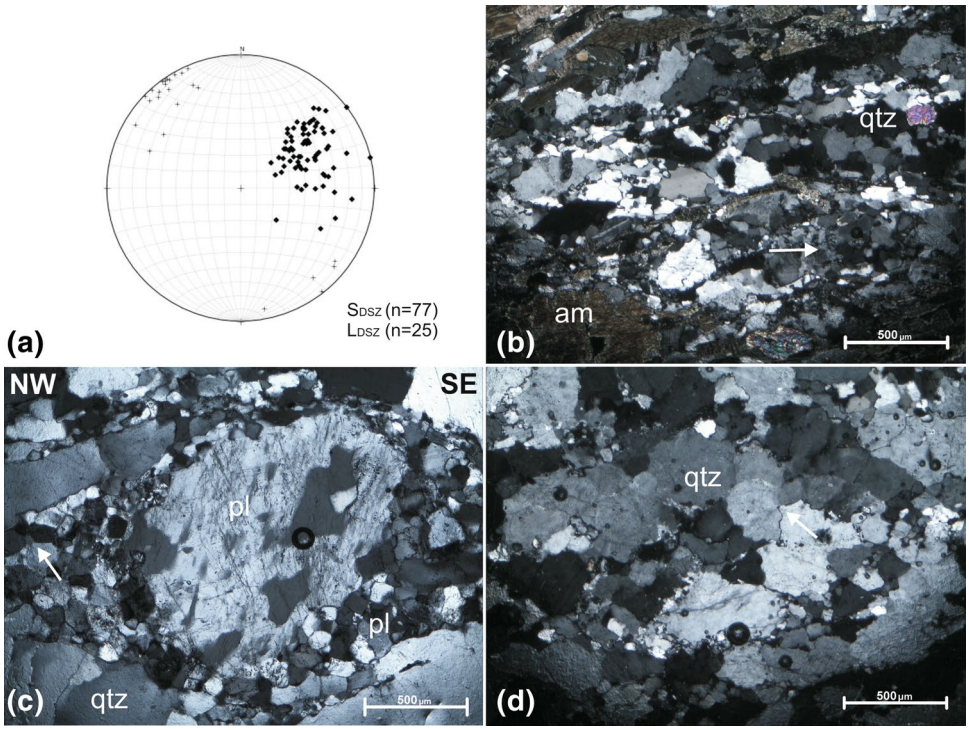

Fig. 11 Microstructural characteristics of the deformation in the Dodov-vrah Shear Zone: **a** lower hemisphere equal area stereoplot of the main metamorphic foliation (S_{DSZ}) and stretching lineation (L_{DSZ}); **b** lobate grain boundaries of quartz due to grain boundary migration recrystallization in meta-diorite (sample NWR-48); **c** core-and-mantle structure of plagioclase, with patchy extinction in the core, in mylonitized pegmatite from a Dodov-vrah Shear Zone. Some of the plagioclase grains in the mantle have a polygonal texture of the boundaries (arrow) which is typical for annealing. Bands of large quartz grains with irregular boundaries alternate with bands of smaller plagioclase grains; **d** small quartz grains along the boundaries of the larger ones in a mylonitized pegmatite from the Dodov-vrah Shear Zone are formed during subgrain rotation dynamic recrystallization as well as low-temperature bulging of the grain boundaries (arrow). The latter are related to the later greenschist-facies conditions

structure (Fig. 12a) corresponds to magmatic growth zoning with large uniform central zone of higher CL intensity (euhedral core) and oscillatory zoned envelope of decreasing CL intensity towards the outer zone. Partial modification of magmatic zircon is apparent in transgressive CL dark domains of pervasive recrystallization, which overprinted oscillatory zonation and affected some cores (grains No 6 and 15), or in resorbed grains overgrown by inhomogeneous CL dark rims (grains No 20 and 23). Such modification should be ascribed to the final stages of magmatic crystallization or to secondary reworking and local new growth by high-T reactions, deformation, and/or fluid ingress (Corfu et al. 2003; Harley et al. 2007). The results of 29 analysed spots in 18 zircon grains yielded concordant $^{207}Pb/^{235}U$–$^{206}Pb/^{238}U$ ages at 10% filter in the range of 74.7–174.7 Ma (Table 1 of the supplementary material) with a spread in U–Pb data along or near the concordia curve (Fig. 12b). The majority of them, representing magmatic growth zoning, range from 149 to 166 Ma with a weighted average age of 156.4 ± 2.5 Ma (an inset in Fig. 12b) and relatively uniform Th/U ratio values (0.19–0.48; average 0.27). Although considered concordant, these data did not define a single satisfactory concordant age of the magmatic protolith. We accept the weighted average of 156.4 ± 2.5 Ma for the orthogneiss magmatic protolith. Six results, which date domains of recrystallization and new growth, cluster between 74 and 86 Ma. The Th/U ratio values of these are low (0.02–0.09; except for one case with Th/U 0.91). Three of these data points yield a concordant age of 81.7 ± 0.68 Ma (Fig. 12c), indicating a metamorphic overprint at amphibolite-facies conditions (*for the interpretation see chapter Discussion*). The data with intermediate ages of 125–141 Ma (Fig. 12b) are considered mixed ages, indicative of incomplete recrystallization and Pb loss and hence geologically meaningless.

Sample 15-52 was collected on the northern slopes of the Rila Mountains (N42°12′1.09″, E 23°24′30.29″; Fig. 3a), from a sheared pegmatite–aplite vein within para- and orthogneisses of the Malyovitsa Unit, deformed in the vicinity of the North-Rila Detachment Fault (Fig. 3a, see also chapter 4). The majority of the monazite grains display complex zoning patterns on BSE images. The smaller grains (60–80 µm) are subhedral to ovoid, rarely unzoned, commonly with a combination of sector and concentric zoning, and almost free of inclusions (Fig. 13a). The larger grains

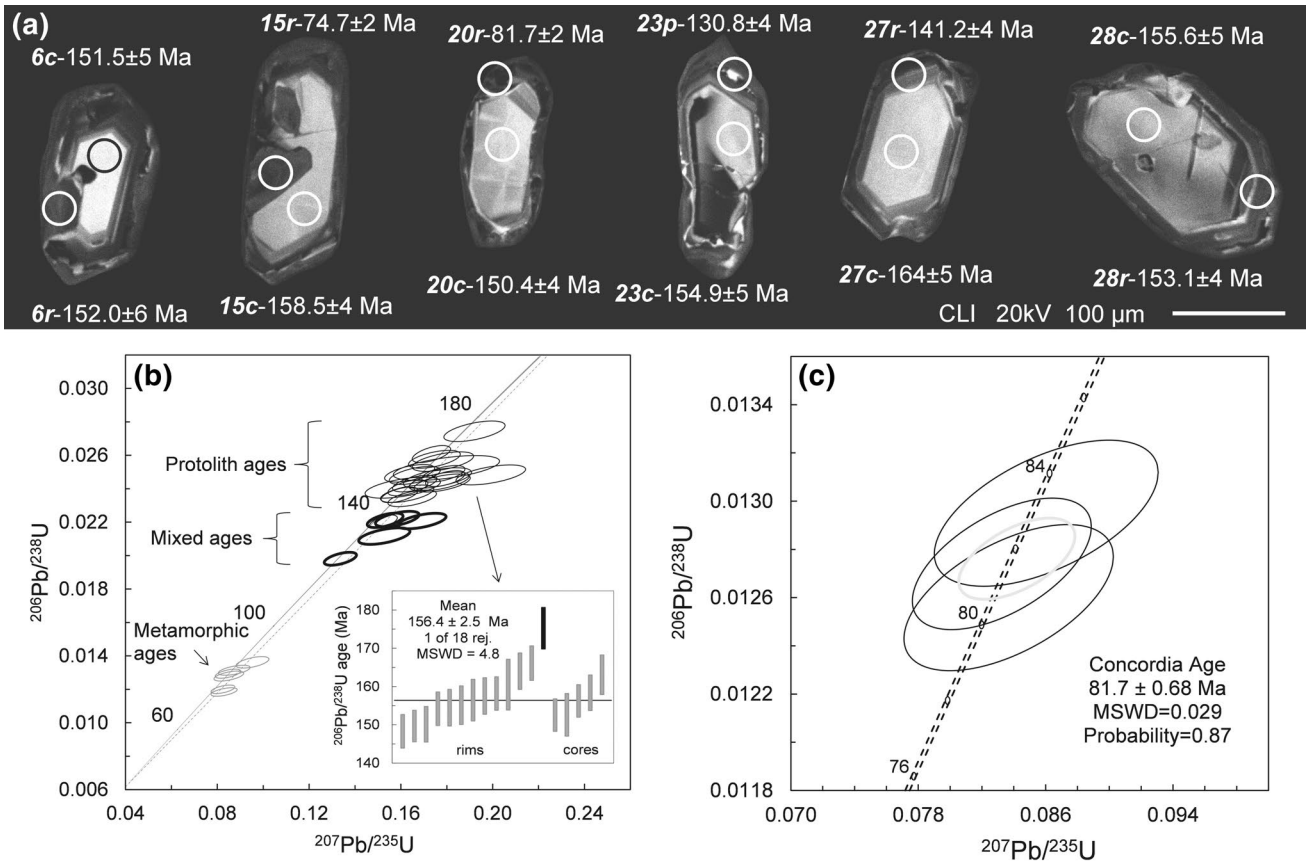

Fig. 12 Zircons from an orthogneiss body in the Malyovitsa Unit, sample NWR-75A: **a** CL images; **b** $^{207}Pb/^{235}U$–$^{206}Pb/^{238}U$ plot with black thin ellipses of protolith ages, black thick ellipses of mixed ages and grey ellipses of metamorphic ages. The inset displays weighted average of protolith ages; **c** Wetherill U–Pb concordia plot of metamorphic zircon data

(150-180 µm) are subhedral to anhedral with a combination of sector, oscillatory and patchy zoning, and numerous inclusions (Fig. 13b).

The U–Th–Pb results of 32 analyses in 11 small and 7 large grains are provided in Table 2 of the supplementary material. The majority of $^{206}Pb/^{238}U$–$^{207}Pb/^{235}U$ ages are discordant. The concordant $^{208}Pb/^{232}Th$–$^{206}Pb/^{238}U$ ages are considered reliable, since ^{232}Th is very abundant in monazites and ^{208}Pb originating from common Pb is negligible compared to radiogenic ^{208}Pb. Fifteen $^{208}Pb/^{232}Th$–$^{206}Pb/^{238}U$ results are concordant at 3% filter (Fig. 13c) and plot in the range of 46.6–55.0 Ma, with most frequent values of 50 to 53 Ma. Six results from small and large grains, yielded a concordant $^{206}Pb/^{238}U$–$^{207}Pb/^{235}U$ age of 51.3 ± 0.66 Ma (Fig. 13d). This age corresponds probably to abundant monazite growth in the pegmatite-aplite vein.

The zircon grains from sample 15–52 are subhedral to anhedral with numerous inclusions of quartz, feldspars and probably U-rich phases (see Fig. 14a). All grains exhibit heterogeneous patchy internal texture and low to moderate CL emission due to metamictization (Fig. 14a). Such texture is commonly due to metasomatic replacement of zircon during a late magmatic stage or subsequent metamorphism (Corfu et al. 2003). The studied zircons are U-rich (2399–10155 ppm), with strongly variable Th contents (87–9292 ppm) and Th/U ratio values (0.03–1.54; < 0.06 mostly, see Table 3 of the supplementary material). The majority of measured spots produced strongly discordant ages. Three spots only (shown in Fig. 14a) yielded subconcordant ages of 49.9 Ma, 53.2 Ma and 56.7 Ma (see the supplementary material), corresponding partly to the monazite age variation. The Wetherill diagram (Fig. 14b) shows a linear trend that crosscuts the concordia at 51.2 ± 1.9 Ma. We consider this result meaningful for zircon formation in view of coinciding age of the monazite (51.3 ± 0.66 Ma; Fig. 13d).

The summarized results indicate a timespan of about 3 Ma for mineral crystallization and subsequent partial resetting at solidus or subsolidus conditions. A simplified interpretation for the age of the pegmatite-aplite vein (sample 15–52) is ~ 51 Ma.

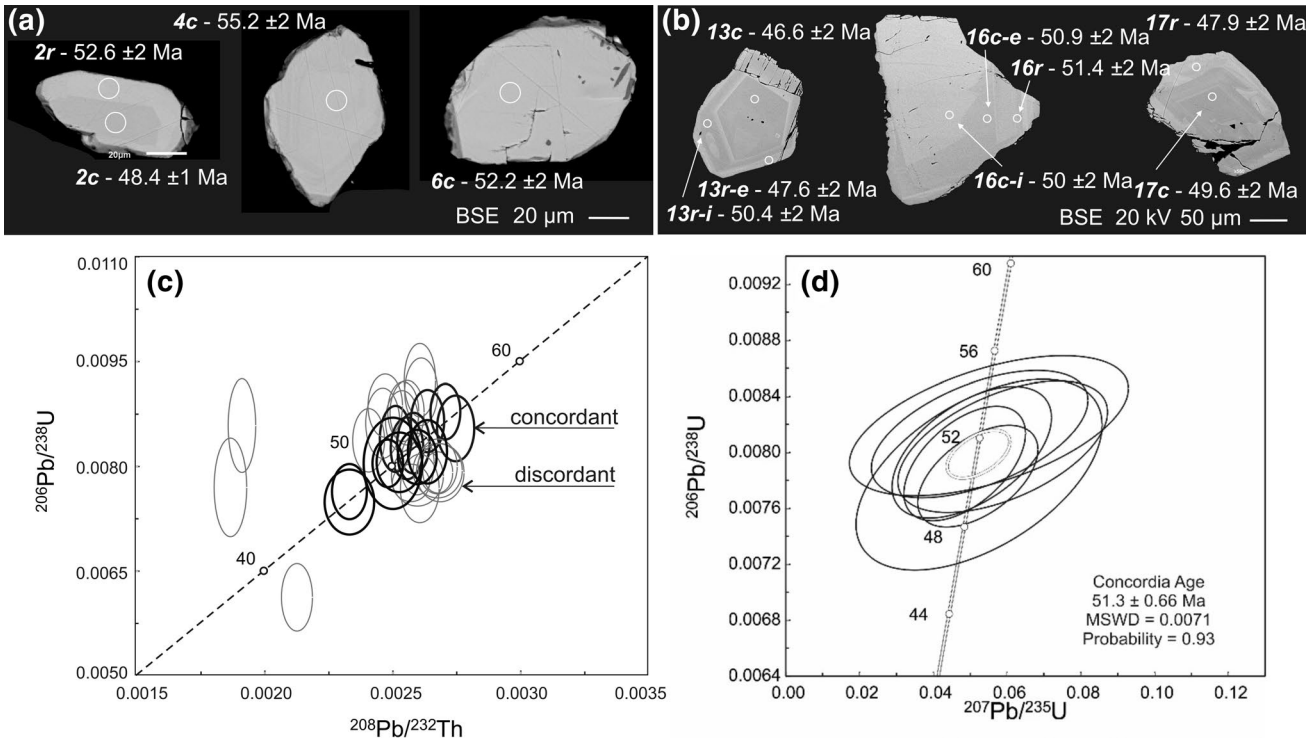

Fig. 13 Monazites from a syn-kinematic pegmatite-aplite (sample 15–52): **a** BSE images of smaller grains (60–80 µm); **b** BSE images of larger grains (150–180 µm); **c** $^{208}Pb/^{232}Th$–$^{206}Pb/^{238}U$ isochron with thick ellipses of concordant data at 3% filter and thin ellipses of discordant data not considered in the interpretation, and an inset of mean concordant $^{208}Pb/^{232}Th$ age for small and large grains; **d** Wetherill concordia plot. All data-point error symbols are 1σ

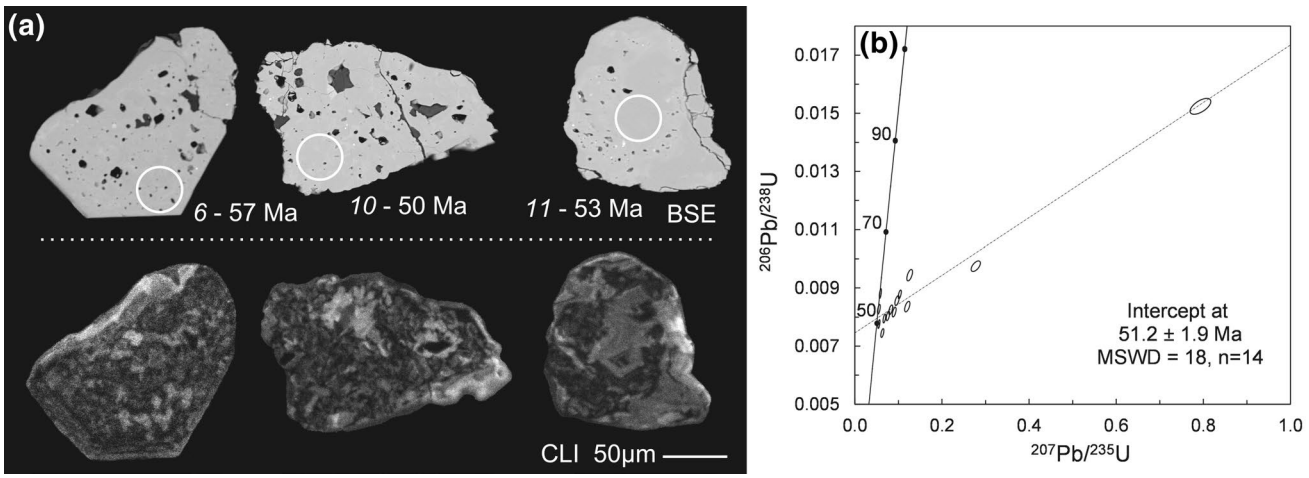

Fig. 14 Zircons from a ductile-sheared pegmatite-aplite vein, sample 15–52: **a** BSE images above and CL images below, showing abundant inclusions, patchy zonation and analytical spots with ages; **b** concordia plot showing linear trend with the lower intercept age of the zircon formation (ellipses plotted with a 1σ error)

Age constrains for the Kabul Unit

Sample NWR-6 was collected from a deformed plagioclase-rich pegmatite (N42°11′2.40″, E23°17′50.20″) hosted by migmatised garnet-bearing schists in the lower section of the Kabul Unit. The separated zircons are euhedral, prismatic to long-prismatic. CL images display magmatic growth zoning with a broad uniform central zone and a complex sector and oscillatory zoned envelope (Fig. 15a). Domains of penetrative recrystallization are very rare. The results of 68 analysed

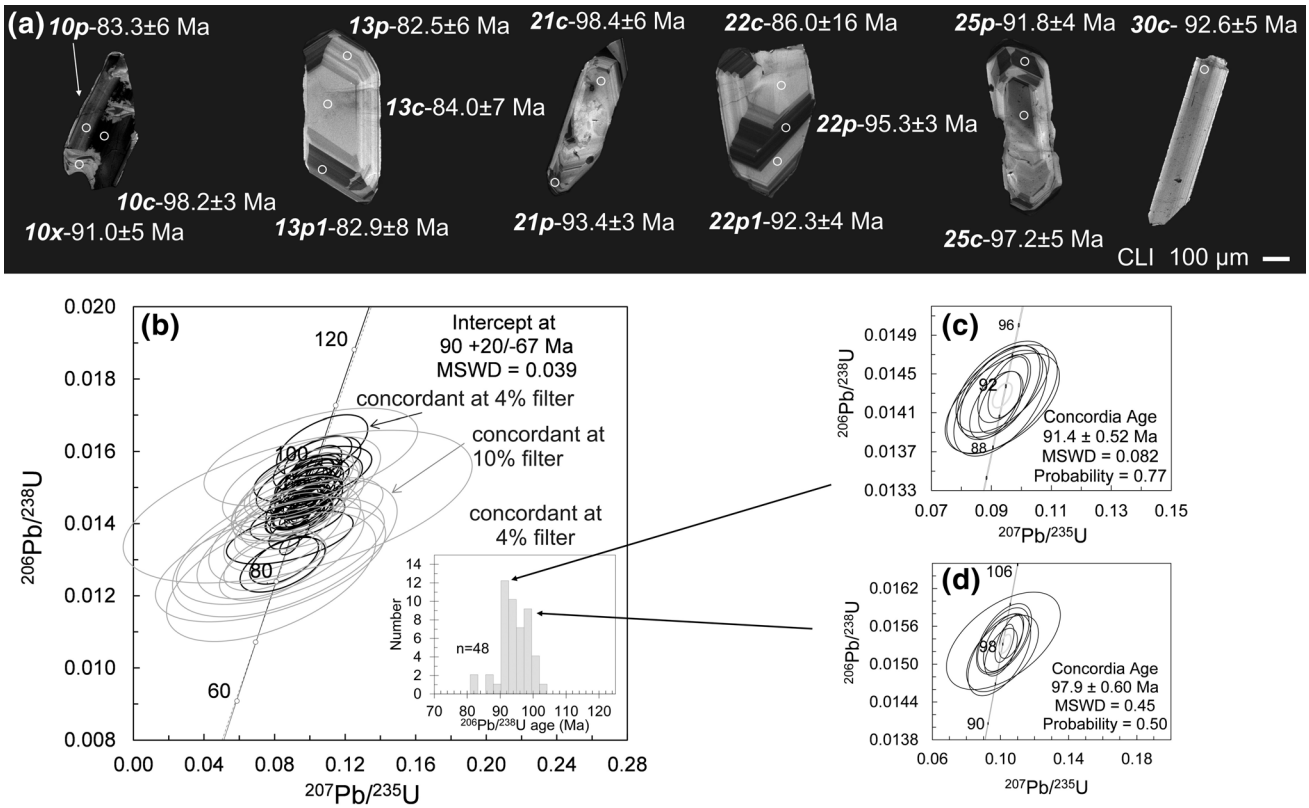

Fig. 15 Zircons from a deformed pegmatite within schists in the Kabul Unit, sample NWR-6: **a** CL images; **b** concordia plot with grey ellipses for concordant ages at 10 % filter and black ellipses for concordant ages at 4 % filter. The inset shows a histogram of concordant ages at 4 % filter with two age peaks; **c** Wetherill U–Pb concordia plot of the most frequent ages in the cluster of older age peak; **d** Wetherill U–Pb concordia plot of the most frequent ages with concordance 100% in the group of younger data

spots in 30 grains yielded concordant ages at 10% filter in the range of 81.1 to 103.4 Ma (Fig. 15b, Table 4 of the supplementary material). The majority of them (48 analyses of discordance < 4%) show two overlapping age clusters (an inset in Fig. 15b) with the most frequent values in the range of 90–92 Ma and 98–100 Ma averaging 91.4 ± 0.52 Ma (ten spots) (Fig. 15c); and 97.9 ± 0.60 Ma (nine spots), respectively (Fig. 15d). Most of the Th/U ratio values are below 0.15 with average of 0.07. The homogeneous central zones and their zoned envelops do not show systematic differences with respect to age and Th/U values. Though two of the measurements are in recrystallized domains, their results do not deviate from the above mentioned ages and Th/U values. The growth zoning of zircon supports a magmatic origin of the dated pegmatite. The subsequent metamorphic stages did not cause noticeable zircon recrystallization and isotope resetting. Hence, the age of the last metamorphic event (M_{K-3}) in Kabul Unit is younger than 91 Ma.

Sample NWR-48 (N42°11′29.48″, E23°18′47.31″) was collected from a sill-like meta-diorite body in the lowest section of the Kabul Unit (Fig. 3a). The separated zircons are prismatic with slightly rounded outlines. They display broad central zones (cores) of weak CL emission and complex sector and oscillatory zoned rims with stronger CL emission (Fig. 16a) corresponding to growth zoning in magmatic zircons (Corfu et al. 2003). Few grains contain CL dark domains of penetrative recrystallization. Both cores and zoned rims show similar Late Cretaceous ages. The U–Pb results of 30 analyses in 22 grains are given in Table 5 of the supplementary material. The majority of the data ($n = 18$) are concordant at 10% filter (Fig. 16b) in the range of 68.90–82.33 Ma with a mean of 75.4 ± 1.2 Ma (Fig. 16c). The zircon rims show slightly older ages than the zircon core. The concordant age of four analysed spots in the rims is 76.2 ± 0.61 Ma (Fig. 16d) and the concordant age of four spots in the cores is 73.8 ± 0.68 Ma (Fig. 16e). The reason for reversed age differences may be loss of radiogenic Pb in the cores. The older concordant ages (rim ages) are likely to represent crystallization ages. Th/U ratio values (0.13–0.73, mean 0.50, in the supplementary material) support magmatic zircon origin. There is no correlation between $^{206}Pb/^{238}U$ ages, Th and U contents, and Th/U ratio values. We consider the age of 76.2 ± 0.61 Ma determined for rims to be the age of diorite body formation.

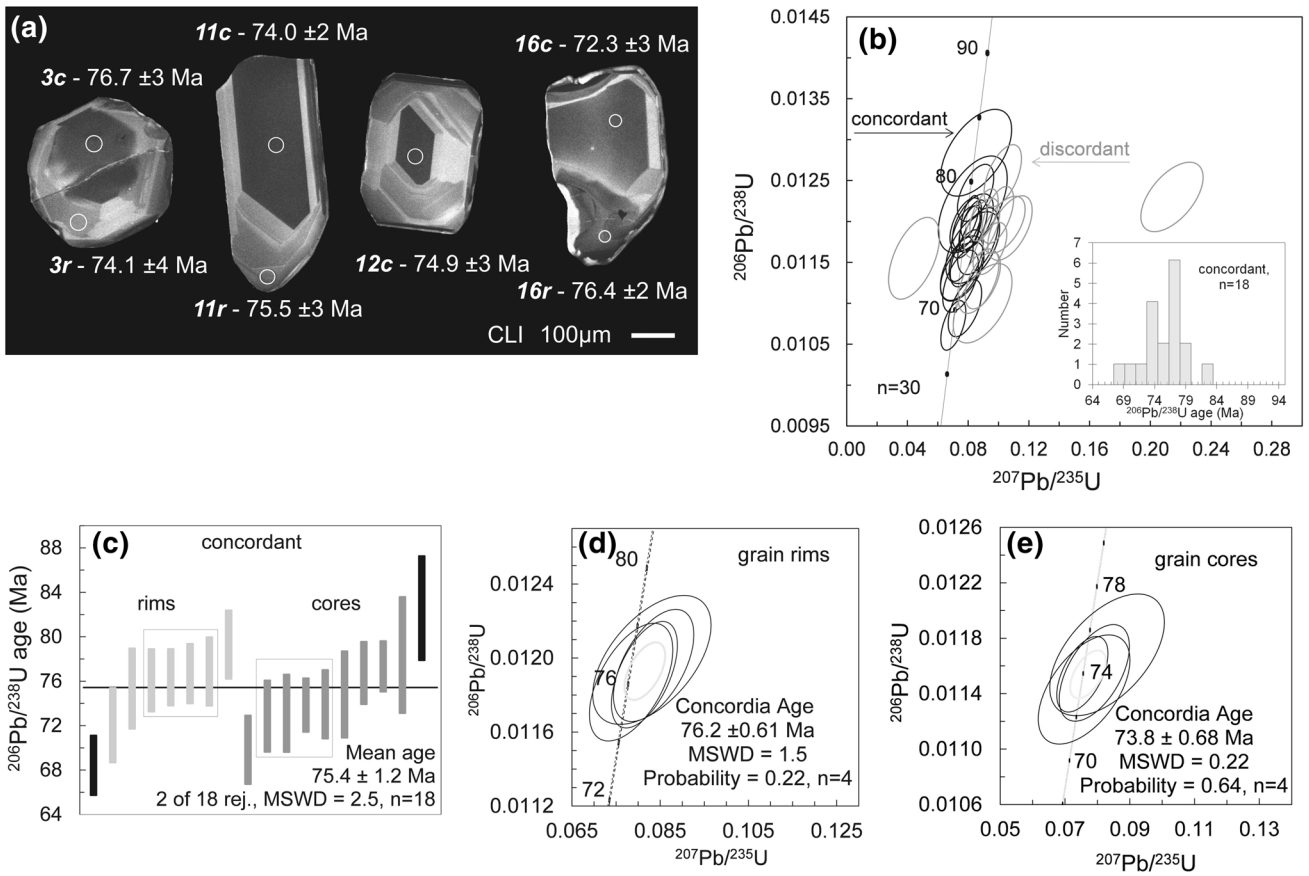

Fig. 16 Zircons from a sill-like meta-diorite body, sample NWR-48: **a** CL images; **b** concordia diagram with grey ellipses of discordant data not considered in the interpretation and black ellipses of concordant data at 100 ± 10% filter. The inset shows histogram of the concordant $^{206}Pb/^{238}U$ zircon ages; **c** mean concordant $^{206}Pb/^{238}U$ ages of rims and cores. **d** Wetherill U–Pb concordia plot of zircon rims from **c**; **e** Wetherill U–Pb concordia plot of zircon cores from **c**

Sample NWR-138 (N42°10′56.21″, E23°15′34.60″) was collected from the biotite granite of the Kalin Pluton. The zircon grains (size 100–200 μm) are euhedral, prismatic to long-prismatic, and free of inclusions. The CL images reveal magmatic growth zoning with a large uniform central zone and oscillatory zoned envelope (Fig. 17a). CL-bright domains of recrystallization disrupt concentric oscillatory zoned rims (grains No 2, 5). They formed probably during late and post-magmatic cooling. Several grains contain xenocrystic cores, some of them with complex internal texture and irregular outlines (grains No 3, 6). The U–Pb results of 39 analyses in 25 grains are provided in Table 6 of the supplementary material. The majority of the results cluster around 60 Ma (Fig. 17b) with deviation from the concordia line (Fig. 17c). Th/U ratio values vary from 0.07 to 1.57 (mean 0.36). The ages of concordant data at 3% filter are in the range of 57.23 to 62.27 Ma. Seven of them yielded a concordant age of 60.40 ± 0.32 Ma (an inset in Fig. 17c) which we interpret as crystallization age of the biotite granite. The xenocrystic cores yielded variable concordant and discordant ages from 68 to 458 Ma (Fig. 17b), part of which should be considered mixed ages.

Age constrains for the activity of Dodov-vrah Shear Zone

Sample NWR-78 was collected from a syn-to-late-kinematic aplite vein, emplaced within the Dodov-vrah Shear Zone (N42°12′47.78″, E23°18′5.67″; Fig. 3a). Monazite and zircon crystals were separated for dating. The monazite population consists of euhedral to subhedral grains and fragments. BSE images reveal concentric oscillatory zoning (Fig. 18a). The U–Th–Pb results of 43 analyses in 18 grains (100–200 μm size) are given in Table 7 of the supplementary material. Twelve results with a variation of 44.6–50.9 Ma for $^{208}Pb/^{232}Th$ ages and 43.8–55.1 Ma for $^{206}Pb/^{238}U$ ages correspond to concordance at 3% filter and cluster around 48 Ma (Fig. 18b). Six of them yield a concordant $^{206}Pb/^{238}U$–$^{207}Pb/^{235}U$ age of 47.9 ± 0.80 Ma (Fig. 18c).

The scanty zircon population in sample NWR-78 consists of small grains (50–100 μm). The CL images (not shown)

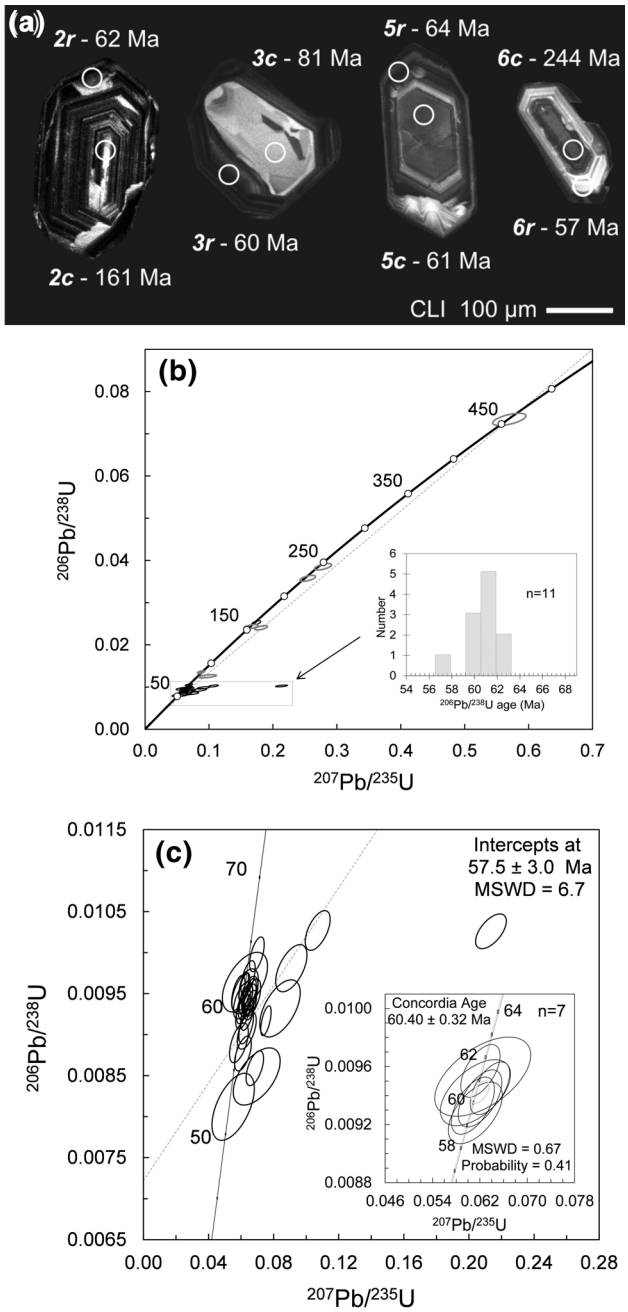

Fig. 17 Zircons from the Kalin pluton biotite granite (sample NWR-138): **a** CL images; **b** concordia plot with all the analyses. Most of them cluster around 60 Ma (black ellipses) corresponding to the histogram peak of 60–62 Ma (an inset in Fig. 17b). The xenocrystic cores (grey ellipses) tend towards older ages; **c** Wetherill U–Pb concordia plot with results around 60 Ma and an inset of concordant ages at 3 % filter

display dark xenocrystic cores mantled by irregular rims of recrystallization or new zircon growth, which are too thin for LA-ICP MS analyses. The xenocrystic cores yielded variable subconcordant $^{206}Pb/^{238}U$ ages in the range of 300–2286 Ma (see Table 8 of the supplementary material). We interpret these zircons as being inherited due to low solubility which is a common feature of felsic low-temperature undersaturated melts (Miller et al. 2003; Boehnke et al. 2013).

Based on the results of monazite dating the age of 48 Ma can be accepted as the time of late-kinematic aplite vein crystallization of sample NWR-78.

Discussion

Interpretation of the local geology

Our field studies and structural analysis show that the Dodov-vrah Shear Zone is a first-order tectonic boundary within the Rhodope Metamorphic Complex, which juxtaposes units with distinct tectono-metamorphic evolutions (Figs. 2, 3, 19). The pervasive structures developed in the footwall and the hanging wall of the Dodov-vrah Shear Zone show opposite kinematics. The shear zone is here interpreted as a major thrust that juxtaposes older and higher grade rocks in the hanging wall (Kabul Unit) against younger and lower grade rocks in the footwall (Malyovitsa Unit). Although highly strained, the rocks from both the footwall and the hanging wall of the shear zone have preserved structures and mineral assemblages from their earlier tectono-metamorphic history.

The ages of the eclogite (Miladinova et al. 2013) and granulite to high-temperature amphibolite-facies assemblages (Kolcheva and Cherneva 1999; Machev 2002), registered within the rocks of Kabul Unit are not well established. The protolith age of the amphibolites from the lower section of Kabul Unit, that contains also eclogites, is ca. 265 Ma. The questionable age of ca. 235 Ma for the eclogite-facies (Miladinova et al. 2013) corresponds to the age of ca. 238 Ma, obtained for the granulite to high amphibolite-facies leucosomes, hosted in the same section of the unit (Gorinova et al. 2015a). Thus, the ages obtained for both the eclogites and the granulites may well show a transition from high-pressure to high-temperature conditions due to exhumation, an interpretation suggested already by previous authors (Kolcheva and Cherneva 1999; Machev 2002). The structural studies show that the pegmatite veins (*Sample NWR-6*) which intruded into the Kabul Unit at ca. 91 Ma were deformed at 500-650 °C during the formation of the main metamorphic fabric of the unit S_{K-m}. Hence, the main penetrative foliation of Kabul Unit was formed during a separate top-to-the northwest tectono-metamorphic event but not during a single clockwise path following the high-pressure and high-temperature events. Due to the same style and mechanisms of deformation as well as same kinematics of the Kabul Unit and the overlying Bistritsa Shear Zone and Polich Unit, we interpret the high-grade penetrative S_{K-m}/L_{K-m} fabric and the associated top-to-the

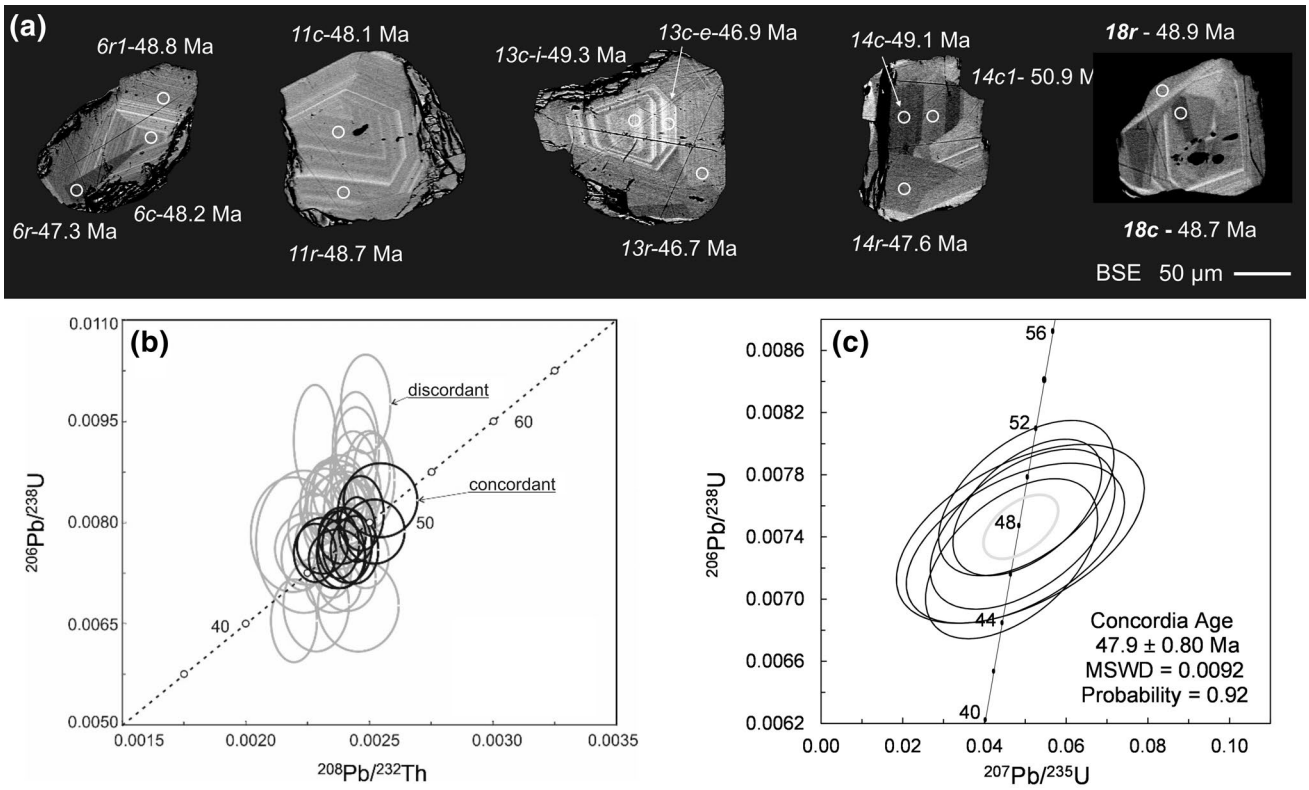

Fig. 18 Monazites from a syn-kinematic aplite vein in the paragneisses of the Malyovitsa Unit (sample NWR-78). **a** BSE images; **b** $^{208}Pb/^{232}Th$–$^{206}Pb/^{238}U$ plot with black ellipses of concordant data at 3% filter and grey ellipses of discordant data not considered in the interpretation. **c** Wetherill concordia plot of the most frequent ages. Data-point error ellipses are 1σ

north-northwest shearing as related to the emplacement of the Polich Unit onto the Kabul Unit along the top-to-the-northwest Bistritsa Shear Zone. The age of this shearing along the Bistritsa Shear Zone and attendant pervasive fabric in the Kabul Unit is ca. 91 Ma or younger (i.e., the final crystallization age of the sheared pegmatites, *sample NWR-6*) and older than the 60 Ma post-kinematic Kalin Pluton (Sample NWR-138). These fabrics were certainly formed before the thrusting of Kabul onto Malyovitsa Unit, since the structures typical for the entire Kabul Unit are folded and overprinted by the mylonitic fabric related to Dodov-vrah Shear Zone. The age and kinematics of the Bistritsa Shear Zone allow some orogen-scale correlations with similar structures from the high-grade basement of Osogovo–Lisets Complex (Kounov et al. 2004) located to the west and northwest of the study area. The Osogovo–Lisets Complex is composed of migmatised gneisses and amphibolites that after the migmatisation were overprinted by regional metamorphism and top-to-the north shearing at moderate amphibolite-facies conditions (Kounov et al. 2004). The north-facing tectonic transport was interpreted as related to the Lower Cretaceous compressional event (100-90 Ma) that finally shaped the Early Alpine orogeny in this part of the Balkan peninsula (Kounov et al. 2004). The similarity of timing and kinematics allows us to interpret the thrusting along Bistritsa Shear Zone and the formation of the main metamorphic fabric in Kabul Unit as elements of the Late Lower Crateceous to Early Upper Cretaceous Orogen (Fig. 19c) preserved in the area of Rila Mountains.

The relative age of the older fabrics within the Malyovitsa Unit may be inferred from the relationships of pre- and post-kinematic intrusive rocks that are hosted by the rocks of the unit. There is no information available about the protolith ages of rocks from the upper variegated section of Malyovitsa Unit, but these should be considered older than the included orthogneiss bodies with a protolith age of ca. 156 Ma (*sample NWR-75A*). Due to the presence of older S_{M-1} foliation and its similar style of deformation and isoclinal folding in both the lower orthogneiss and the upper variegated sections, we interpret this fabric to be younger than the protolith age of the orthogneisses (156-135, see Von Quadt et al. 2006; Peytcheva et al. 2007; Popov and Ivanov 2012). The Malyovitsa Unit hosts also Late Cretaceous plutons (72–70 Ma; see Von Quadt and Peytcheva 2005; Peytcheva et al. 2007) that do not contain isoclinal folds and were overprinted by later fabrics such as S_{M-2}/L_{M-2} and S_{NRD}/L_{NRD}. A concordia age of ca. 82 Ma obtained from recrystallised rims of zircon crystals

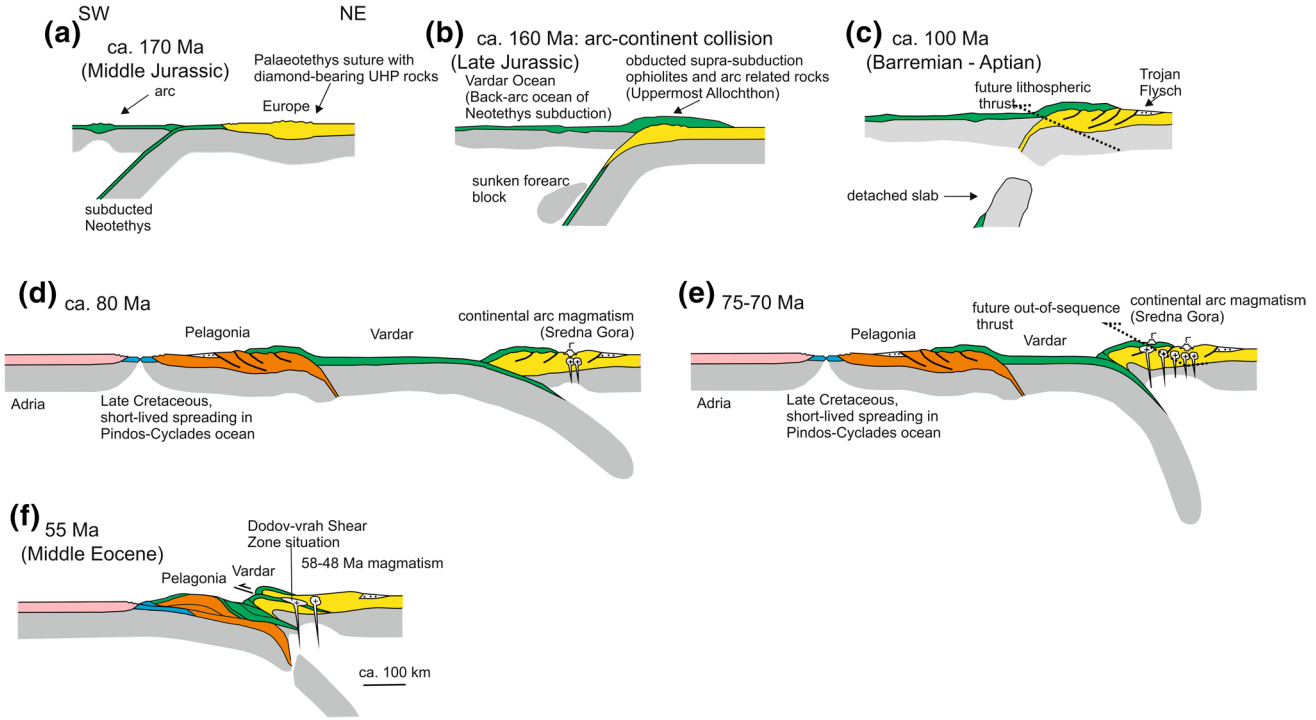

Fig. 19 Schematic tectonic model showing tectonic evolution of the Rhodope Metamorphic Complex and in particular, the evolution and position of the Dodov-vrah Shear Zone as a first-rank tectonic boundary, separating the Upper and the Middle Allochthons in the northwestern parts of the Rhodope Metamorphic Complex. The model is adopted from Froitzheim et al. (2014), with minor changes: **a** Southward subduction of the Neotethys triggers formation of an island arc south of the European plate in Middle Jurassic time. **b** Subduction is followed by obduction of the Jurassic arc and adjacent oceanic crust (together forming the Uppermost Allochthon) onto the European continental margin (Upper Allochthon) in Late Jurassic time. **c** During the Early Cretaceous and after the obduction, the end of the convergence caused formation of a north verging fold-and-thrust belt with flysch troughs in the foreland. At the same time, the subducted European (Moesian) slab was detached and sank in the mantle. **d** New northward subduction of the Vardar oceanic crust below Europe (i.e., the newly formed active European continental margin, including the Late Jurassic–Early Cretaceous Orogen) led to the formation of a Late Cretaceous volcanic arc (for example, in Sredna Gora Tectonic Zone). Meanwhile, the Vardar oceanic crust was obducted also onto Pelagonia. **e** Subduction of the Vardar oceanic crust as well as the arc magmatism in Sredna Gora Zone continued over the entire Late Cretaceous (the last pulses were dated at 68–70 Ma. **f** In Middle Eocene time, due to the final closure of the Vardar Ocean, Europe (containing also the Late Cretaceous volcanic arc), collided with Pelagonia. This extreme compression caused a top-to-the southeast (for the Rila Mountains area) out of sequence thrusting of the European margin (i.e., the Upper and the Uppermost allochthons) onto rocks that before the thrusting were also parts of the same units (i.e., Uppermost and Upper allochthons). Thus, large parts of the Upper and the Uppermost allochthons were tectonically reburied and formed parts of the presently known Middle Allochthon

from the dated Jurassic orthogneiss body (*sample NWR-75A*) is interpreted as indicating an amphibolite-facies metamorphic event. Therefore, we interpret the formation of S_{M-1} as related to a tectono-metamorphic event in the Late Cretaceous (see Fig. 19d), most probably in the course of subduction of the Vardar Ocean beneath the active continental margin of Europe. The penetrative S_{M-2} and L_{M-2} are younger than the Late Cretaceous plutons hosted by the Malyovitsa Unit (i.e., younger than ca. 70 Ma). The upper age limit of these structures is fixed by the age of the crosscutting ca. 42 Ma biotite granites of the Rila–Rhodope Batholith (Peytcheva et al. 1998). Since the temperature conditions, style of deformation, and kinematics within the rocks of the Malyovitsa Unit and those affected by the Dodov-vrah Shear Zone are similar, we suggest that the origin of the penetrative S_{M-2}/L_{M-2} fabric is contemporaneous with the age of thrusting along the Dodov-vrah Shear Zone and formation of its mylonitic fabric.

The age of the Dodov-vrah Shear Zone is revealed by the age (48–49 Ma) of syn-kinematic granitic dykes and veins. Pairs of folded and stretched dykes as well as presence of tension joints filled with the same granitic material show that during their emplacement the shear zone was active. The similar ages (48 and 51 Ma) of two granite samples with different structural position within the Malyovitsa Unit (aplite—sample NWR-78 from the Dodov-vrah Shear Zone and pegmatite-aplite—sample 15–52 from the lower orthogneiss section, respectively), show that this type of felsic magmatism was typical for the entire Malyovitsa Unit. The 3 Ma difference in age shows that the magmatic activity was relatively long lasting but not a single magmatic pulse.

Since the formation of the main fabric in the Malyovitsa Unit is considered as contemporaneous with the activity of Dodov-vrah Shear Zone, we interpret the upper age limit for the formation of S_{M-2}/L_{M-2} between 51 and 48 Ma. The onset of the thrusting along the shear zone is unknown but it must be considered younger than ca. 70 Ma, the age of the sheared Late Cretaceous plutons.

Regional geology correlations

The Malyovitsa Unit contains orthogneisses with Late Jurassic and Early Cretaceous magmatic protolith ages (155–150 Ma in Von Quadt et al. 2006; Peytcheva et al. 2007; ~ 135 Ma in Popov and Ivanov 2012) that overlap with ages of orthogneisses from units of the Rhodope Metamorphic Complex that were interpreted as parts of the of the Middle Allochthon (Turpaud 2006; Turpaud and Reischmann 2010; Von Quadt et al. 2008; Cherneva et al. 2011; Froitzheim et al. 2014). Therefore, the Malyovitsa Unit should be considered as a coherent part of the Middle Allochthon. Moreover, due to the lack of migmatisation, the Malyovitsa Unit should be considered as a part of the upper, lower grade (non-migmatic) nappe of the Middle Allochthon.

In Late Palaeocene–Early Eocene time (56–52 Ma), the Middle Allochthon was intruded by several plutonic bodies (Spanchevo, Dolno Dryanovo, Barutin-Buinovo, Elatia-Skaloti, Pripek), for some of which a syn-kinematic emplacement was suggested (Veit et al. 2003; Jahn-Awe et al. 2010). Most of these were deformed in the course of the continuing top-to-the south thrusting (Jahn-Awe et al. 2010) or later top-to-the north extensional shearing (Jahn-Awe et al. 2012). The syn-kinematic emplacement of the Early Eocene plutons within the rocks of the Middle Allochthon was related to the initial stages of thrusting of the Middle onto the Lower Allochthon (Jahn-Awe et al. 2010). In the area of the Western Rhodopes and Pirin Mountains (south of the study area) the emplacement of the Upper Allochthon (Obidim/Vertiskos–Ograzhden Unit) onto the Middle Allochthon (Sidironero–Mesta Unit) was interpreted as older or contemporaneous with the intrusion of the 55 Ma old Dolno Dryanovo Pluton (Georgiev et al. 2010). However, the present-day boundary between Upper and Middle allochthons (i.e., Obidim/Vertiskos–Ograzhden and Sidironero–Mesta units) in that part of the Rhodope Metamorphic Complex, represents a Late Eocene–Early Oligocene extensional detachment fault (Georgiev et al. 2010). Similar is the tectonic situation in the eastern and northeastern parts of Chalkidiki peninsula, where the boundary between the Upper Allochthon (Vertiskos Unit) and the Middle Allochthon (Kerdilion Unit) represents the Late Eocene Kerdilion Detachment Fault (Kilias et al. 1999; Georgiev et al. 2010). Therefore, direct correlations between these boundaries and the Dodov-vrah Shear Zone are rather speculative. The Upper Allochthon appears also on wide areas in the Eastern parts of the Rhodope Metamorphic Complex but due to the lack of detailed structural and geochronology studies, there is no clear separation between the Upper and the Middle allochthons in that area. Moreover, in the area of the eastern Rhodopes the existence of the Middle Allochthon is still questionable.

Careful analysis of literature data shows that plutons of 56–52 Ma emplaced within the units of the Middle Allochthon are syn-kynematic with respect to a tectono-metamorphic event that produced the penetrative top-to-the-south fabric within the rocks of the Middle Allochthon. These interpretations are also supported by the age of the last metamorphic event of 55.9 ± 7.2 Ma that affected the Middle Allochthon (Asenitsa Unit), in the Northern Rhodopes east of the study area (von Quadt et al. 2006). Intrusions of slightly older age (58–60 Ma) also occur in the Upper Allochthon (Kalin Pluton dated in this study at 60.4 Ma, or 57.9 Ma according to Zagorchev et al. 2014; and Kapatnik Pluton located south of the study area and dated at 56–58 Ma, see Milovanov et al. 2010). However, the Late Paleocene plutons in the Upper Allochthon are consistently post-kinematic, since they cut the pervasive metamorphic fabric of the host rocks (i.e., S_{K-m} foliation of Kabul Unit). The Kapatnik Pluton (not shown in Figs. 1 and 3) was only sheared at its base (deeper structural levels) and together with its host metamorphic rocks was thrusted towards the south onto lower units of the Rhodope Metamorphic Complex (Gerdjikov 2012). The lack of Late Paleocene and Eocene plutons within the Lower Allochthon would rather show that their emplacement in the Middle Allochthon happened probably at the very beginning of the collision between the Middle and the Lower Allochthons, i.e., probably at the time of subduction of the distal parts of the continental margin (i.e., the Lower Allochthon).

Due to the syn-kinematic character of the granitic dykes and veins within the Dodov-vrah Shear Zone, we agree that the shearing between the two allochthons was still active at 48–50 Ma. Although the only clear post- S_{M-2} and L_{M-2} features in the section of the Middle Allochthon are the Middle Eocene granites of the Rila–Rhodope Batolith (42–37.5 Ma; see Von Quadt and Peytcheva 2005; Gerdjikov et al. 2010), we suggest that the last movements along Dodov-vrah Shear Zone took place at ca. 48 Ma. Thus, the emplacement of the melts dated at 48 Ma (*sample NWR-78*) should reflect the final stages of shearing along the Dodov-vrah Shear Zone and the emplacement of the Upper Allochthon (Kabul Unit) onto the Middle Allochthon (Malyovitsa Unit) of the Rhodope Metamorphic Complex in Northwest Rila. The same kinematics and age of syn-kinematic intrusions within the Middle Allochthon show that the thrusting of the Upper onto

the Middle Allochthon in the western parts of the Rhodope Metamorphic Complex lasted between 58 and 48 Ma.

Conclusions

Field studies, structural analysis and isotope geochronology show that the shearing along the Dodov-vrah Shear Zone lasted between 58 and 48 Ma. Due to the emplacement of older and higher grade metamorphic rocks onto younger and lower grade metamorphic rocks, the Dodov-vrah Shear Zone is interpreted as a thrust structure that juxtaposes units of the Upper Allochthon against units of the Middle Allochthon of the Rhodope Metamorphic Complex. Thus, the Dodov-vrah Shear Zone should be considered a first-order tectonic boundary between major units of the Rhodope Metamorphic Complex. This study shows that even at higher structural levels, top-to-the-south compressional tectonics in the Rhodope Metamorphic Complex were active between the Latest Paleocene and the Middle Eocene and that the main top-to-the-south syn-compressional structure of the nappe edifice was formed by that time. The study area covers only a limited part at the northwestern Rhodope Metamorphic Complex but the results and interpretations presented here can be applied as a model of the polyphase tectono-metamorphic evolution of other parts of the Rhodope Metamorphic Complex.

Acknowledgements We are grateful to Niko Froitzheim, Jan Pleuger, Thorsten Nagel and Valerie Bosse for the fruitful discussions. We also thank Fernando Corfu and the anonymous reviewer for their constructive remarks and suggestions, which have improved this manuscript considerably. This study is supported by the National Science Fund of Bulgaria, Grant number 03/58 and by Elatzite-Med Ltd.

Funding This work was funded by Bulgarian National Science Fund (03/58) and Elatzite-Med Ltd. (3191).

References

Aleinikoff JN, Schenck WS, Plank MO, Srogi L, Fanning CM, Kamo SL, Bosbyshell H (2006) Deciphering igneous and metamorphic evens in high-grade rocks of the Wilmington Complex, Delaware: morphology, cathodoluminescence and backscattered electron zoning, and SHRIMP U-Pb geochronology of zircon and monazite. Geol Soc Am Bull 118:39–64

Arnaudov V (1975) Pegmatite types of various ages from the northwestern part of the Rhodope Massif. Geol Balc 5(4):59–72

Arnaudov V, Pavlova M, Amov B, Baldjieva T (1974) Age and genesis of pegmatites from Southern Bulgaria: Pb isotopic data of their feldspars. In Mineral Genesis, Sofia, pp 315-331 (in Bulgarian)

Arnaudov V, Amov B, Baldjieva TS, Pavlova M (1990) Tertiary migmatic pegmatites in the Central Rhodope crysstalline complex. Uranium–lead zircon dating. Geol Balc 20(6):25–32

Boehnke P, Watson EB, Trail D, Harrison TM, Schmitt AK (2013) Zircon saturation re-revisited. Chem Geol 351:324–334

Bonev N, Stampfli G (2003) New structural and petrologic data on Mesozoic schists in the Rhodope (Bulgaria): geodynamic implications. C R Geosci 335:691–699

Bonev N, Stampfli G (2008) Petrology, geochemistry and geodynamic implications of Jurassic island arc magmatism as revealed by mafic volcanic rocks in the Mesozoic low-grade sequence, eastern Rhodope, Bulgaria. Lithos 100:210–233

Bonev N, Burg J-P, Ivanov Z (2006) Mesozoic-Tertiary structural evolution of an extensional gneiss dome—the Kesebir-Kardamos dome, eastern Rhodope (Bulgaria-Greece). Int J Earth Sci 95:318–340

Bonev N, Spiking R, Moritz R, Marchev P (2010a) The effect of Alpine thrusting in late-stage extensional tectonics: evidence from the Kulidzhik nappe and the Pelevun extensional allochthon in the Rhodope Massif, Bulgaria. Tectonophysics 488:256–281

Bonev N, Spiking R, Moritz R, Marchev P (2010b) Timing of extensional exhumation of the Eastern Rhodope high-grade basement (Bulgaria): 40Ar/39Ar age constraints. In: National conference geoscience proceedings, Sofia, pp 117–118

Bosse V, Boulvais P, Gautier P, Tiepolo M, Ruffet J, Devidal L, Cherneva Z, Gerdjikov I, Paquette JL (2009) Fluid-induced disturbance of the monazite Th-Pb chronometer: in situ dating and element mapping in pegmatites from the Rhodope (Greece, Bulgaria). Chem Geol 261:286–302

Burchfiel BC, Nakov R, Tzankov T (2003) Evidence from the Mesta half-graben, SW Bulgaria, for the Late Eocene beginning of Aegean extension in the Central Balkan Peninsula. Tectonophysics 375:61–76

Burg J-P (2012) Rhodope: from Mesozoic convergence to Cenozoic extension. Review of petro-structural data in the geochronological frame. J Virtual Explor. https://doi.org/10.3809/jvirtex.2011.00270

Burg J-P, Ivanov Z, Ricou L-E, Dimov D, Klain L (1990) Implications of shear-sense criteria for the tectonic evolution of the Central Rhodope Massif, southern Bulgaria. Geology 18:451–454

Burg J-P, Godfriaux I, Ricou L-E (1995) Rhodope thrust units in the Vertiskos–Kerdilion Massif (Northern Greece). C R Acad Sci (Paris) 320:889–896

Burg J-P, Ricou L-E, Ivanov Z, Godfriaux I, Dimov D, Klain L (1996) Syn-metamorphic nappe complex in the Rhodope Massif. Structure and kinematics. Terra Nova 8:6–15

Carrigan C, Mukasa S, Haydoutov I, Kolcheva K (2006) Neoproterozoic magmatism and Carboniferous highgrade metamorphism in the Sredna Gora Zone, Bulgaria: an extension of the Gondwana-derived Avalonian-Cadomian belt? Precambr. Res 147(3–4):404–416

Cherneva Z, Kolcheva K, Arnaudova R (1998) Petrological and geochemical characteristics of metagranites from Northwestern Rila Mt. Geochem Miner Pet 33:73–90

Cherneva Z, Ovtcharova M, Dimov D, von Quadt A (2006) Baby-granites" in migmatites from Chepinska river valley, Western Rhodope—geochemistry and U–Pb isotope dating on monazite and zircon. In: National conference geosciences proceedings, Sofia, pp 205–208

Cherneva Z, Boyanova V, Peytcheva I, Naydenov K, Stefanova E (2011) P-T conditions and time of migmatization in the southwestern part of the Rhodope metamorphic terrain (Slashten unit). In: National conference geosciences proceedings, Sofia, pp 47–48

Collings D, Savov I, Maneiro K, Baxter E, Harvey J, Dimitrov I (2016) Late Cretaceous UHP metamorphism recorded in kyanite–garnet schists from the Central Rhodope Mountains, Bulgaria. Lithos. 246–247:165–181. https://doi.org/10.1016/j.lithos.2016.01.002

Corfu F, Hanchar JM, Hoskin PW, Kinny P (2003) Atlas of zircon textures. Rev Mineral Geochem 53:469–500

Didier A, Bosse V, Cherneva Z, Gautier P, Georgieva M, Paquette JL et al (2014) Syn-deformation fluid-assisted growth of monazite during renewed high-grade metamorphism in metapelites of the Central Rhodope (Bulgaria, Greece). Chem Geol 381:206–222

Dimitrova E (1960) Petrology of crystalline basement of Northwestern Rila Mountain. Trav Geol Bulg Ser Geochem Met Nonmet 1:199–257

Dimov D, Damyanova K (1996) Synmetamorphic tecotnic units in Northwest Rila. Rev Bulg Geol Soc 57(2):25–30

Dimov D, Georgiev N (2000) Exhumation related milonitization of granitoids—an example from the Rila-Rhodope Batholith. Ann Univ Sofia 92(1):23–27

Dinter DA (1998) Late Cenozoic extension of the Alpine collisional orogen, northeastern Greece: origin of the north Aegean basin. Geol Soc Am Bull 110:1208–1226

Dinter D, Royden L (1993) Late Cenozoic extension in northeastern Greece: Strymon Valley detachment and Rhodope metamorphic core complex. Geology 21:45–48

Froitzheim N, Jahn-Awe S, Frei D, Wainwright AN, Maas R, Georgiev N, Nagel TJ, Pleuger J (2014) Age and composition of meta-ophiolite from the Rhodope Middle Allochthon (Satovcha, Bulgaria): a test for the maximum-allochthony hypothesis of the Hellenides. Tectonics. https://doi.org/10.1002/2014tc003526

Gautier P, Bosse V, Cherneva Z, Didier A, Gerdjikov I, Tiepolo M (2017) Polycyclic alpine orogeny in the Rhodope metamorphic complex: the record in migmatites from the Nestos shear zone (N. Greece). Bull Soc Geol Fr 188(6):36

Georgiev N, Pleuger J, Froitzheim N, Sarov S, Jahn-Awe S, Nagel TJ (2010) Separate Eocene-Early Oligocene and Miocene stages of extension and core complex formation in the Western Rhodopes, Mesta Basin, and Pirin Mountains (Bulgaria). Tectonophysics 487:59–84

Georgiev N, Froitzheim N, Cherneva Z, Frei D, Grozdev V, Jahn-Awe S, Nagel TJ (2016) Structure and U-Pb zircon geochronology of an Alpine nappe stack telescoped by extensional detachment faulting (Kulidzhik area, Eastern Rhodopes, Bulgaria). Int J Earth Sci 105(7):2171–2173

Gerdjikov I (2012) Penetrative shearing in the southern part of Kapatnik pluton: possible tectonic implications. In: National conference geosciences proceedings, Sofia, pp 105–106

Gerdjikov I, Gautier P, Cherneva Z, Ruffet G (2006) The northwestern segment of the North Rhodopean extensional system and related fabrics in the Rila-Rhodopean Batholith. In: National conference geosciences proceedings, Sofia, 79–82

Gerdjikov I, Gautier P, Cherneva Z, Bosse V, Ruffet G (2010) Late Eocene synmetamorphic thrusting and synorogenic extension across the metamorphic pile of the Bulgarian Central Rhodope. In: XIX Congress of the Carpathian Balkan geological association, Thessaloniki, Greece, 23–26 September 2010, abstract volume 132–133

Gorinova TS, Georgiev N (2015) Lithotectonic units in the metamorphic basement of NW Rila, Bulgaria. In: National conference geosciences proceedings, Sofia, pp 91–92

Gorinova TS, Peychev K, Georgiev N, Cherneva Z, Kiselinov H, Georgiev S, Peytcheva I (2014) Structural and U/Pb zircon age data from Rila and Vlachina Mountains: implications for tectonic correlations of basement units from SW Bulgaria. Bul Shk Gjeol 1(2014):319

Gorinova TS, Cherneva Z, Georgiev N, Peytcheva I (2015a) Dating of garnet-bearing leucosome from NW Rila Mountain, Bulgaria. In: National conference geosciences proceedings, Sofia, pp 61–62

Gorinova TS, Georgiev N, Cherneva Z, Grozdev V (2015b) Kinematics and age of thrusting of the Upper onto the Lower Allochthon of the Rhodope Metamorphic Complex. An example from NW Rila Mt., Bulgaria. In National conference GEOSCIENCES proceedings, Sofia, pp 93–94

Griffin WL, Powell WJ, Pearson NJ, O'Reilly SY (2008) GLITTER: data reduction software for laser ablation ICP-MS. In Laser Ablation ICP-MS in the Earth Sciences: Current practices and outstanding issues (Sylvester P., ed.). Mineral Assoc Can Short Course Series 40:307–311

Harley SL, Kelly NM, Möller A (2007) Zircon behaviour and the thermal histories of mountain chains. Elements 3:25–30

Himmerkus F, Reischmann T, Kostopoulos D (2009) Triassic rift-related meta-granites in the Internal Hellenides, Greece. Geol Mag 146:252–265

Ivanov Z (1988) Aperçu general sur l'évolution géologique et structurale du massif des Rhodopes dans lae cadre des Balkanides. Bull Soc Géol, France 2:227–240

Ivanov Z (1989) Structure and tectonic evolution of the central parts of the Rhodope massif. In: Ivanov Z (ed) Guide to excursion E-3, CBGA-XIV congress. Sofia, Bulgaria

Ivanov Z (2017) Tectonics of Bulgaria. Sofia University Press, Sofia **(in Bulgarian with English resume)**

Jackson S, Pearson N, Griffin W, Belousova E (2004) The application of laser ablation-inductively coupled plasma-mass spectrometry to in situ U–Pb zircon geochronology. Chem Geol 211:47–69

Jahn-Awe S, Froitzheim N, Nagel TJ, Frei D, Georgiev N, Pleuger J (2010) Structural and geochronological evidence for Paleogene thrusting in the Western Rhodopes, SW Bulgaria: elements for a new tectonic model of the Rhodope Metamorphic Province. Tectonics 29:TC3008. https://doi.org/10.1029/2009tc002558

Jahn-Awe S, Pleuger J, Frei D, Georgiev N, Froitzheim N, Nagel T (2012) Time constraints for low-angle shear zones in the Central Rhodopes (Bulgaria) and their significance for the exhumation of high-pressure rocks. Int J Earth Sci 101:1971–2004

Janák M, Froitzheim N, Georgiev N, Nagel TJ, Sarov S (2011) P-T evolution of kyanite eclogite from the Pirin Mountains (SW Bulgaria): implications for the Rhodope UHP Metamorphic Complex. J Metamorph Geol 29:317–332

Jaranoff, D (1960) La tectonique de la Bulgarie. Sofia, Technica (in Bulgarian, abstract in French)

Kauffmann G, Kockel F, Mollat H (1976) Notes on the stratigraphic and paleogeographic position of the Svoula Formation in the innermost zone of the Hellenides (Northern Greece). Bull Soc Geol Fr 18:225–230

Kilias A, Falalakis G, Mountrakis D (1999) Cretaceous-Tertiary structures and kinematics of the Serbomacedonian metamorphic rocks and their relation to the exhumation of the Hellenic hinterland (Macedonia, Greece). Int J Earth Sci 88:513–531

Kirchenbaur M, Pleuger J, Jahn-Awe S, Nagel TJ, Froitzheim N, Fonseca ROC, Münker C (2012) Timing of high-pressure metamorphic events in the Bulgarian Rhodopes from Lu-Hf garnet geochronology. Contrib Miner Pet 163:897–921

Kolcheva K, Cherneva Z (1999) Metamorphic evolution of metapelites from the North-western Rila mountain. Geochem, Miner Pet 36:45–66

Kounov A, Seward D, Bernoulli D, Burg J-P, Ivanov Z (2004) Thermotectonic evolution of an extensional dome: the Cenozoic Osogovo-Lisets core complex (Kraishte Zone, W Bulgaria). Int J Earth Sci 93:1008–1024. https://doi.org/10.1007/s00531-004-0435-2

Krenn K, Bauer C, Proyer A, Klötzli U, Hoinkes G (2010) Tectonometamorphic evolution of the Rhodope orogen. Tectonics 29:TC4001. https://doi.org/10.1029/2009tc002513

Kronberg P (1969) Gliederung, Petrographie und Tektogenese des Rhodopen-Kristllin in Tsal-Dag Simvolon und Ost-Pangäon (Griechische Makedonien). Geotekt Forsch 31:1–49

Liati A (2005) Identification of repeated Alpine (ultra) high-pressure metamorphic events by U–Pb SHRIMP geochronology and REE

geochemistry of zircon: the Rhodope zone of Northern Greece. Contrib Mineral Petr 150:608–630
Liati A, Theye T, Fanning CM, Gebauer D, Rayner N (2015) Multiple subduction cycles in the Alpine orogeny, as recorded in single zircon crystals (Rhodope zone, Greece). Gondwana Res. https://doi.org/10.1016/j.gr.2014.11.007
Ludwig KR (2012) A Geochronological Tolkit for Microsoft Excel: Berkeley Geochronology Center Special Publication 5
Machev PH (2002) Metabasites from Kabul mixed complex (Western Rila Mountain)—magmatic and metamorphic evolution. In: National conference geosciences proceedings, Sofia, pp 8–10
Marchev P, Filipov P (2012) First findings of Late Cretaceous magmatic rocks in Pirin Mts. In: National conference geosciences proceedings, Sofia, pp 55–56
Marchev P, von Quadt A, Peytcheva I, Ovtcharova M (2006) The age and origin of the Chuchuliga and Rozino granites, Eastern Rhodopes. In National conference geosciences proceedings, Sofia 2006, pp 213–216
Miller CF, McDowell SM, Mapes RW (2003) Hot and cold granites? Implications of zircon saturation temperatures and preservation of inheritance. Geol 31(6):529–532
Milovanov P, Petrov I, Marinova A, Ilieva E, Peytcheva I, Von Quadt A, Pristavova S (2010) New geological and geochronological data of granitic and metamorphic rocks from SW Bulgaria. Geol Balc 39(1–2):256
Mposkos E, Wawrzenitz N (1995) Metapegmatites and pegmatites bracketing the time of HP-metamorphism in polymetamorphic rocks of the E. Rhodope, northern Greece: petrological and geochronological constraints. Geol. Soc. Greece, Spec Publ 4:602–608
Mposkos E, Krohe A, Baziotis I (2010) Alpine polyphase metamorphism in metapelites from Sidironero complex (Rhodope domain, NE Greece). In: Proceedings of the 19th Congress of the CBGA, Thessaloniki, Greece, 100:173–181
Miladinova I, Froitzheim N, Sandmann S, Nagel, TJ, Georgiev N, Münker C (2013) Middle Triassic eclogite in the Rila Mountains (Rhodope Upper Allochton, Bulgaria): A vestige of Palaeotethys subduction. Alpine Workshop 2013, Schladming, Austria
Nagel TJ, Schmidt S, Janák M, Froitzheim N, Jahn-Awe S, Georgiev N (2011) The exposed base of a collapsing wedge—the Nestos Shear Zone (Rhodope Metamorphic Province, Greece). Tectonics 30:TC4009. https://doi.org/10.1029/2010tc002815
Okay A, Satır M, Tüysüz O, Akyüz S, Chen F (2001) The tectonics of the Strandja Massif: late-Variscan and mid-Mesozoic deformation and metamorphism inthe northern Aegean. Int J Earth Sci 90:217–233
Ovtcharova M, von Quadt A, Cherneva Z, Peytcheva I, Heinrich C A, Kaiser-Rohrmeier M, Neubauer F, Frank M (2003) Isotope and geochronological study on magmatism and migmatization in the Central Rhodopian core complex, Bulgaria. In: Neubauer F, Handler R (eds) Geodynamics and ore deposit evolution of the Alpine-BalkanCarpathian-Dinaride Province. ABCD—GEODE Workshop Proceedings, Seggauberg, Austria, p 42
Ovtcharova M, von Quadt A, Cherneva Z, Sarov S, Heinrich C, Peytcheva I (2004) U-Pb dating of zircon and monazite from granitoids and migmatites in the core and eastern periphery of the Central Rhodopean Dome, Bulgaria. Geochim Cosmochim Acta 68:A664
Passchier CW, Trouw RAJ (2005) Microtectonics, 2nd edn. Springer, Berlin, p 366. ISBN-10 3-540-64003-7
Petrik I, Janak M, Froitzheim N, Georgiev N, Yoshida K, Sasinkova V, Konecny P, Milovska S (2016) Triassic to Early Jurassic (c. 200 Ma) UHP metamorphism in the Central Rhodopes: evidence from U–Pb–Th dating of monazite in diamond-bearing gneiss from Chepelare (Bulgaria). J Metam Geol 34:265–291. https://doi.org/10.1111/jmg.12181
Peytcheva I, Kostitsin Y, Salnikova E, Kamenov B, Klain L (1998) Rb–Sr and U–Pb isotope data for the Rila-Rhodope Batholith. Geochem Miner Pet 35:3–27 **(in Bulgarian)**
Peytcheva I, von Quadt A, Ovtcharova M, Handler R, Neubauer F, Salnikova E, Kostitsyn Yu, Sarov S, Kolcheva K (2004) Metagranitoids from the eastern parts of the Central Rhodopean Dome (Bulgaria): U–Pb, Rb–Sr and 40Ar/39Ar timing of emplacement and exhumation and isotope-geochemical features. Miner Pet 82:1–31. https://doi.org/10.1007/s00710-004-0039-3
Peytcheva I, von Quadt A, Naydenov K, Sarov S, Dimov D, Voinova E (2007) U–Pb zircon-xenotime-monazite dating and Hf-isotope tracing to distinguish Cretaceous and Paleogene granitoids in the Western Rhodopes and Rila Mountain. In: National conference geosciences proceedings, Sofia, pp 89–91 (with Bulgarian abstract)
Peytcheva I, von Quadt A, Sarov S, Voinova E, Kolcheva K (2009) Ordovician protoliths of metamorphic rocks in Eastern Pirin—Western Rhodopes: Are they part of the Ograzhden Unit? In: National conference geosciences proceedings, Sofia, pp 17–18
Pleuger J, Georgiev N, Jahn-Awe S, Froitzheim N, Valkanov N (2011) Kinematics of Palaeogene low-angle extensional faults and basin formation along the eastern border of the Central Rhodopes (Bulgaria). Z Dtsch Ges Geowiss 162:171–192
Popov M, Ivanov I (2012) Two contrasting U–Pb zircon age determinations of metamorphic rocks in the western part of the Rhodope metamorphic complex. In: National conference Geosciences proceedings, Sofia, 63–64
Raeva E, Peytcheva I, Ovtcharova M, Cherneva Z (2008) U–Pb zircon dating of granites and orthogneisses from the madan unit in the arda river valley, Central Rhodopes, Bulgaria. Geosciences, 37–38
Ricou LE, Burg JP, Godfriaux I, Ivanov Z (1998) Rhodope and Vardar: the metamorphic and the olistostromic paired belts related to the Cretaceous subduction under Europe. Geodin Acta 11:285–309
Sarov (2012) Lithotectonic subdivision of the metamorphic rocks in the area or Rila and Rhodope Mountains—results from geological mapping at scale 1:50 000. In: International conference The school of Prof Zivko Ivanov, pp 43–47
Sarov S, Voynova E, Moskovski S, Jelezarski T, Naydenov K, Nikolov D, Georgieva I, Nedkova K, Petrov N, Markov N (2007) Map sheet K-35-86-V (Arda). Explanatory note to the Geological map of the Republic of Bulgaria scale 1:50,000, Sofia
Sarov S, Voynova E, Moskovski S, Jelezarski T, Georgieva I, Nikolov D, Naydenov K, Nedkova K, Petrov N, Markov N, Marinova R (2008a) Geol. map of the Rep. Bulg., scale 1:50,000, Map sheet K-35-74-V (Chepelare). Explanatory note to the Geological map of the Republic of Bulgaria scale 1:50,000, Sofia
Sarov S, Voynova E, Moskovski S, Jelezarski T, Georgieva I, Nikolov D, Naydenov K, Nedkova K, Petrov N, Markov N, Marinova R (2008b) Map sheet K-35-74-G (Davidkovo). Explanatory note to the Geological map of the Republic of Bulgaria scale 1:50,000, Sofia
Sarov S, Yordanov B, Georgieva S, Valkov V, Balkanska E, Grozdev V, Markov N, Marinova R (2008c) Map sheets K-35-87-V (Zlatograd) and K-35-99-A (Drangovo). Explanatory note to the Geological map of the Republic of Bulgaria scale 1:50,000, Sofia
Sarov S, Moskovski S, Jelezarski T, Voinova E, Nikolov D, Georgieva I, Markov N (2011a) Map sheet K-34-71-A (Dupnitsa). Explanatory note to the Geological map of the Republic of Bulgaria scale 1:50,000, Sofia
Sarov S, Moskovski S, Jelezarski T, Voynova E, Nikolov D, Georgieva I, Valev V, Markov N (2011b) Map Sheet K-34-71-B (Sapareva banya). Explanatory note to the Geological map of the Republic of Bulgaria scale 1:50,000, Sofia

Sarov S, Voynova E, Nikolov D, Georgieva I.,Valev V, Markov N (2011c) Map Sheet K-34-71-G (Rilski manastir). Explanatory note to the Geological map of the Republic of Bulgaria scale 1:50,000, Sofia

Sarov S, Moskovski S, Jelezarski T, Voynova E, Nikolov D, Georgieva I,Valev V, Markov N (2011d) Map Sheet K-34-71-V (Blagoevgrad). Explanatory note to the Geological map of the Republic of Bulgaria scale 1:50,000, Sofia

Schmidt S, Nagel TJ, Froitzheim N (2010) A new location with microdiamond-bearing metamorphic rocks south of Sidironero (SW Rhodopes/Greece). Eur J Mineral 22:189–198. https://doi.org/10.1127/0935-1221/2010/0022-1999

Seydoux-Guillaume AM, Wirth R, Nasdala L, Gottschalk M, Montel JM, Heinrich W (2002a) An XRD, TEM and Raman study of experimentally annealed natural monazite. Phys Chem Min 29:240–253

Seydoux-Guillaume AM, Paquette JL, Wiedenbeck M, Wiedenbeck M, Montel JM, Heinrich W (2002b) Experimental resetting of the U–Th–Pb systems in monazite. Chem Geol 191(1–3):165–181

Shipkova KA (1999) Synmetamorphic deformations in the NW Rila mountain. Dissertation, Sofia University (in Bulgarian)

Shipkova K, Ivanov Z (2000) The Djerman Detachment fault—an effect of the late Tertiary extension in the north-west part of the Rhodope Massif. C R Acad Bulg Sci 53(2):81–84

Slama J, Kosler J, Crowley JL, Gerdes A, Hanchar J, Horstwood M, Morris GA, Nasdala L, Norberg N, Schaltegger U, Tubrett MN, Whitehouse MJ (2008) Plešovice zircon—a new natural reference material for U–Pb and Hf isotopic microanalysis. Chem Geol 249:1–35

Soldatos T, Koroneos A, Kamenov BK, Peytcheva I, von Quadt A, Christofides G, Zheng X, Sang H (2008) New U–Pb and Ar–Ar mineral ages for the Barutin-Buynovo-Elatia-Skaloti-Paranesti batholith (Bulgaria and Greece): refinement of its debatable age. Geochem Miner Pet 46:85–102

Trouw RAJ, Passchier CW, Wiersma DJ (2010) Atlas of Mylonites and Related Structures. Springer, Berlin

Tueckmantel C, Schmidt S, Neisen M, Georgiev N, Nagel TJ, Froitzheim N (2008) The Rila-Pastra Normal Fault and multi-stage extensional unroofing in the Rila Mountains (SW Bulgaria). Swiss J Geosci 101:295–310

Turpaud P (2006) Characterization of igneous terranes by zircon dating: implications for the UHP relicts occurrences and suture identification in the Central Rhodope, Northern Greece. Unpublished Dissertation, Johannes-Gutenberg-Universität, Mainz

Turpaud P, Reischmann T (2010) Characterisation of igneous terranes by zircon dating: implications for UHP occurrences and suture identification in the Central Rhodope, northern Greece. Int J Earth Sci 99:567–591

Veit B, Kruhl JH, Machev P (2003) Multiple syntectonic granitoid intrusions during the Alpine development of the Rhodope Massif (southern Bulgaria): preliminary results. Neues Jahrb Geol Palaeontol Abh 228:321–341

Von Quadt A, Peytcheva I (2005) The southern extension of the Srednogorie type Upper Cretaceous magmatism in Rila-Western Rhodopes: constraints from isotope-geochronological and geochemical data. In: Proc Jubilee Intern Conf 80 years BGS, Sofia, pp 113–116

Von Quadt A, Sarov S, Peytcheva I, Voynova E, Petrov N, Nedkova K, Naydenov K (2006) Metamrphic rocks from northern parts of Central Rhodopes—conventional and in situ U–Pb zircon dating, isotope tracing and correlations. In: Proc Joint Conf Bulg Geoph Geol Soc "Geosciences 2006", pp 225-228

Von Quadt A, Peytcheva I, Sarov S, Naydenov K, Georgiev N (2008) Metamorphic rocks from Dospat area of Western Rhodopes—conventional and in situ U-Pb zircon dating, isotope tracing and correlations. In: National conference GEOSCIENCE proceedings, Sofia, pp 33–34

Wetherill GW (1956) Discordant uranium–lead ages. Trans Am Geophys Union 37:320–327

Yordanov B, Sarov S, Georgiev S, Yanev Y, Valkov V, Balkanska E, Grozdev V, Marinova R, Markov N (2008a) Map sheet K-35-75-V (Komuniga). Explanatory note to the Geological map of the Republic of Bulgaria scale 1:50,000, Sofia

Yordanov B, Sarov S, Georgiev S, Valkov V, Balkanska E, Grozdev V, Marinova R, Markov N (2008b) Map sheet K-35-87-A (Ardino). Explanatory note to the Geological map of the Republic of Bulgaria scale 1:50,000, Sofia

Zagorchev I, Goranov A, Vulkov V, Boyanov I (1999) Palaeogene sediments in the Padala graben, northwestern Rila Mountain, Bulgaria. Geol Balc 29(3–4):57–67

Zagorchev I, Balica C, Kozhoukharova E, Balintoni I, Sabau G, Negulescu E (2014) Palaeogene igneous evolution of the Rhodopes. In: National conference geosciences proceedings, Sofia, pp 35–36

Zidarov N, Nenova P, Dimov V (1995) Coesite in kyanite eclogites from Ograzden Mts, SW Bulgaria. C R Acad Bulg Sci 48(11–12):59–62